

Upper Generalization Bounds for Neural Oscillators

Zifeng Huang^{a,*}, Konstantin M. Zuev^b, Yong Xia^c, Michael Beer^{a,d,e}

^a*Institute for Risk and Reliability, Leibniz University Hannover, Callinstraße 34, Hannover, 30167, Germany*

^b*Department of Computing and Mathematical Sciences, California Institute of Technology, Pasadena, California, United States*

^c*Joint Research Centre for Marine Infrastructure, Department of Civil and Environmental Engineering, The Hong Kong Polytechnic University, Kowloon, Hong Kong, China*

^d*Department of Civil and Environmental Engineering, University of Liverpool, Liverpool, L69 3GH, United Kingdom*

^e*International Joint Research Center for Resilient Infrastructure & International Joint Research Center for Engineering Reliability and Stochastic Mechanics, Tongji University, Shanghai, 200092, China*

Abstract

Neural oscillators that originate from the second-order ordinary differential equations (ODEs) have shown competitive performance in learning mappings between dynamic loads and responses of complex nonlinear structural systems. Despite this empirical success, theoretically quantifying the generalization capacities of their neural network architectures remains undeveloped. In this study, the neural oscillator consisting of a second-order ODE followed by a multilayer perceptron (MLP) is considered. Its upper probably approximately correct (PAC) generalization bound for approximating causal and uniformly continuous operators between continuous temporal function spaces and that for approximating the uniformly asymptotically incrementally stable second-order dynamical systems are derived by leveraging the Rademacher complexity framework. The theoretical results show that the estimation errors grow polynomially with respect to both the MLP size and the time length, thereby avoiding the curse of parametric complexity. Furthermore, the derived error bounds demonstrate that constraining the Lipschitz constants of the MLPs via loss function regularization can improve the generalization ability of the neural oscillator. A numerical study considering a Bouc-Wen nonlinear system under stochastic seismic excitation validates the theoretically predicted power laws of the estimation errors with respect to the sample size and time length, and confirms the effectiveness of constraining MLPs' matrix and vector norms in enhancing the performance of the neural oscillator under limited training data.

Keywords: Neural oscillator, PAC generalization bound, Causal continuous operator, Rademacher complexity, Lipschitz regularization

1. Introduction

Accurately modeling mappings among long sequences or continuous temporal functions is a significant challenge in machine learning, yet it is critical for a wide range of applications in science and engineering. To address this challenge, numerous neural network architectures have been proposed for sequential and functional learning tasks, which includes recurrent neural networks (RNNs) (Rumelhart et al., 1986) and their enhanced variants (Hochreiter and Schmidhuber, 1997; Cho et al., 2014), attention-based architectures (Vaswani et al., 2017), state-space (SS) models (Gu et al., 2020, 2021, 2022), and neural oscillators (Rusch and Mishra, 2020, 2021; Lanthaler et al., 2023; Rusch and Rus, 2024; Huang and Xia, 2025). Originating from ordinary differential equations (ODEs), SS models and neural oscillators combine the fast inference capability of RNNs with the competitive long-range sequence learning performance of attention-based architectures (Gu and Dao, 2023; Rusch and Rus, 2024). Neural oscillators have been theoretically demonstrated to alleviate vanishing and exploding gradient problems (Rusch and Mishra, 2020, 2021) and to ensure stable dynamics in learning long-range dependencies (Rusch and Rus, 2024). Furthermore, numerical

*Corresponding author.

Email addresses: zifeng.huang@irz.uni-hannover.de (Zifeng Huang), kostia@caltech.edu (Konstantin M. Zuev), ceysia@polyu.edu.hk (Yong Xia), beer@irz.uni-hannover.de (Michael Beer)

studies have demonstrated that neural oscillators are capable of accurately learning and modeling the relationships between random dynamic loads and the corresponding responses of complex nonlinear structural systems (Huang and Xia, 2025).

In addition to the empirical success of SS models and neural oscillators in practical applications, advancing their theoretical understanding, especially in quantifying the approximation and generalization bounds of their network architectures, is also a significant issue. Several studies have theoretically investigated the approximation and generalization bounds of SS models. Li et al. (2022) proved an approximation bound for linear RNNs in universally approximating linear, causal, continuous, regular, and time-homogeneous operators between continuous temporal function spaces. Orvieto et al. (2024) derived an approximation bound for the SS models consisting of a time-discrete linear RNN followed by a multilayer perceptron (MLP) in modeling the mappings between finite-length sequences. Liu and Li (2024) derived a probably approximately correct (PAC) upper generalization bound for a linear SS model using the Rademacher complexity. In this bound, the Rademacher complexity constant incorporates the model parameters and the expectation and variance of sub-Gaussian input function processes. Under the constraint that the spectral abscissa of the state matrix is smaller than zero, Honarpisheh et al. (2025) established a length-independent norm-based generalization bound for the selective SS model. Both studies only considered the mappings from input sequences or continuous temporal functions to vector outputs at a final time instant. By leveraging a layer-by-layer Rademacher contraction approach, Rácz et al. (2024) derived a PAC upper generalization bound for a deep SS model consisting of a time-discrete linear RNN followed by an MLP. This bound is still limited to the mappings from input sequences to scalar outputs, and the estimation error (difference between the generalization error and the approximation error) in this generalization bound grows exponentially with the depth of the employed MLP. In addition to these results, the approximation and generalization properties of the traditional RNNs for approximating continuous mappings between continuous temporal function spaces (Hanson and Raginsky, 2020; Hanson et al., 2021; Fermanian et al., 2021; Hanson and Raginsky, 2024) and those for approximating fading memory causal operators of time-discrete sequences (Grigoryeva and Ortega, 2018a,b; Gonon et al., 2020, 2023; Yasumoto and Tanaka, 2025) have been studied. In contrast to SS models, theoretical analyses of the approximation and generalization properties of neural oscillators remain limited. For a neural oscillator architecture consisting of a second-order ODE followed by an MLP, Huang et al. (2025) established its upper approximation bounds for approximating causal continuous operators between continuous temporal function spaces and for approximating stable second-order dynamical systems. The generalization bounds of neural oscillators, however, remain unexplored.

In this study, the neural oscillator consisting of a second-order ODE followed by an MLP is considered. Its upper PAC generalization bound for approximating causal and uniformly continuous operators between continuous temporal function spaces and that for approximating uniformly asymptotically incrementally stable second-order dynamical systems are established. In Section 2, the neural oscillator architecture is introduced, some necessary assumptions are outlined, and the established theoretical approximation bounds of the neural oscillator in Huang et al. (2025) are briefly reviewed. The newly derived theoretical generalization bounds of the neural oscillator are also informally provided in Section 2 to facilitate understanding. In Section 3, the formal statements of two theorems that establish the generalization bounds for the neural oscillator, accompanied by the supporting lemmas essential for their proofs, are provided. These generalization bounds reveal that constraining the Lipschitz constants of the employed MLPs in the loss function can improve the generalization capability of the neural oscillator. In Section 4, a numerical study based on a Bouc-Wen nonlinear system under stochastic seismic excitation validates the power laws of the established estimation errors with respect to the sample size and time length, and confirms that constraining the MLPs' matrix and vector norms can improve performance of the neural oscillator under limited training data.

Notations: For an n -dimensional vector $\mathbf{a} = [a_1, a_2, \dots, a_n]^\top$, its L^r -norm is $|\mathbf{a}|_r = [\sum_{i=1}^n |a_i|^r]^{1/r}$ for $1 \leq r < \infty$ and $|\mathbf{a}|_r = \max_{1 \leq i \leq n} |a_i|$ for $r = +\infty$. $|\mathbf{a}|$ is short for $|\mathbf{a}|_1$. For a matrix $\mathbf{M} = [m_{ij}]_{p \times q}$, its $L^{r,s}$ -norm is $|\mathbf{M}|_{r,s} = \left\| \left[|\mathbf{m}_1|_r, |\mathbf{m}_2|_r, \dots, |\mathbf{m}_q|_r \right]^\top \right\|_s$, where $1 \leq r, s \leq +\infty$ and \mathbf{m}_j is the j th column vector of \mathbf{M} . The L^r -norm of \mathbf{M} is $|\mathbf{M}|_r = \sup_{|\mathbf{a}|_r=1} |\mathbf{M}\mathbf{a}|_r/|\mathbf{a}|_r$. \mathbb{Z} and \mathbb{R} respectively represent the integer and real number spaces. $\lfloor \cdot \rfloor$ and $\lceil \cdot \rceil$ respectively represent the floor and ceiling functions. $\text{Re}(\cdot)$ and $\text{Im}(\cdot)$ respectively represent the real and imaginary parts of a complex number. $\mathbb{R}^{p \times q}$ represents the $p \times q$ -dimensional real matrix space. $f'(t) = df(t)/dt$ and $f''(t) = d^2f(t)/dt^2$. $C_0([0, T]; \mathbb{R}^p)$ represents a p -dimensional real-valued continuous function space defined over $[0, T]$ with respect to L^∞ -norm $\|\cdot\|_{L^\infty}$. For $\mathbf{u}(t) = [u_1(t), u_2(t), \dots, u_p(t)]^\top \in C_0([0, T]; \mathbb{R}^p)$, its L^∞ -norm is $\|\mathbf{u}(t)\|_{L^\infty} = \sup_{t \in [0, T]} |\mathbf{u}(t)|$, $L^\infty[0, t_0]$ -norm $\|\cdot\|_{L^\infty[0, t_0]}$ is $\|\mathbf{u}(t)\|_{L^\infty[0, t_0]} = \sup_{t \in [0, t_0]} |\mathbf{u}(t)|$, and L^2 -norm $\|\cdot\|_{L^2}$ is $\|\mathbf{u}(t)\|_{L^2} = \sqrt{\int_0^T |\mathbf{u}(t)|_2^2 dt}$. Big O notation:

$f(n) = O[g(n)]$ if there exist positive constants c and n_0 such that $f(n) \leq c \cdot g(n)$ for all $n \geq n_0$.

2. Neural Oscillator

A neural oscillator architecture mapping $\mathbf{u}(t) = [u_1(t), u_2(t), \dots, u_p(t)]^\top \in C_0([0, T]; \mathbb{R}^p)$ to $\mathbf{y}(t) = [y_1(t), y_2(t), \dots, y_q(t)]^\top \in C_0([0, T]; \mathbb{R}^q)$ is (Huang et al., 2025)

$$\begin{cases} \mathbf{x}''(t) = \Gamma[\mathbf{x}(t), \mathbf{x}'(t), \mathbf{u}(t)] \\ \mathbf{y}(t) = \Pi[\mathbf{x}(t), \mathbf{u}(0), t] \end{cases} \quad (1)$$

with $\mathbf{x}(0) = \mathbf{x}'(0) = \mathbf{0}$, where $\mathbf{x}(t) = [x_1(t), x_2(t), \dots, x_r(t)]^\top$ is an intermediate r -dimensional real-valued state function, $\Gamma(\cdot)$ and $\Pi(\cdot)$ are two MLPs

$$\Gamma[\mathbf{x}(t), \mathbf{x}'(t), \mathbf{u}(t)] = \mathbf{W}_2 \sigma_\Gamma \left\{ \mathbf{W}_1 [\mathbf{x}^\top(t), \mathbf{x}'^\top(t), \mathbf{u}^\top(t)]^\top + \mathbf{b}_1 \right\} + \mathbf{b}_2, \quad (2)$$

$$\Pi[\mathbf{x}(t), \mathbf{u}(0), t] = \tilde{\mathbf{W}}_{h_\Pi} \sigma_\Pi \left(\dots \sigma_\Pi \left\{ \tilde{\mathbf{W}}_1 [\mathbf{x}^\top(t), \mathbf{u}^\top(0), t]^\top + \tilde{\mathbf{b}}_1 \right\} \right) + \tilde{\mathbf{b}}_{h_\Pi}, \quad (3)$$

\mathbf{W}_i , $i = 1$ and 2 , $\tilde{\mathbf{W}}_j$, $j = 1, 2, \dots, h_\Pi$, are real-valued tunable weight matrices, \mathbf{b}_i and $\tilde{\mathbf{b}}_j$ are real-valued tunable bias vectors, h_Π is the depth of $\Pi(\cdot)$, and $\sigma_\Gamma(\cdot)$ and $\sigma_\Pi(\cdot)$ are respectively the activation functions of $\Gamma(\cdot)$ and $\Pi(\cdot)$. Unless otherwise specified, these two activation functions are set to the Rectified Linear Unit (ReLU) (Nair and Hinton, 2010), defined as $\sigma_\Gamma(x) = \sigma_\Pi(x) = \sigma_{\text{ReLU}}(x) = \max(0, x)$, in this study. The input layer widths of $\Gamma(\cdot)$ and $\Pi(\cdot)$ are denoted as $w_{\Gamma, \text{in}}$ and $w_{\Pi, \text{in}}$, respectively. The output layer widths of $\Gamma(\cdot)$ and $\Pi(\cdot)$ are denoted as $w_{\Gamma, \text{out}}$ and $w_{\Pi, \text{out}}$, respectively. The largest hidden layer widths of $\Gamma(\cdot)$ and $\Pi(\cdot)$ are denoted as w_Γ and w_Π , respectively. The neural oscillator in Eq. (1) can be written as $\mathbf{y}(t) = \Pi \circ \Phi_\Gamma[\mathbf{u}(\tau)](t) = \Pi \{ \Phi_\Gamma[\mathbf{u}(\tau)](t), \mathbf{u}(0), t \}$, where \circ is the composition operator and $\mathbf{x}(t) = \Phi_\Gamma[\mathbf{u}(\tau)](t)$ represents the mapping governed by the second-order ODE in Eq. (1).

Two theoretical approximation bounds of the neural oscillator in Eq. (1), corresponding respectively to the approximation of causal and uniformly continuous operators and that of uniformly asymptotically incrementally stable second-order dynamical systems, have been established in Huang et al. (2025). These two approximation bounds, together with some necessary assumptions and the definition of uniformly asymptotically incrementally stable systems, are summarized below.

Assumption 1: $C_0([0, T]; \mathbb{R}^p)$ with $T \geq 1$ is a Banach space equipped with the L^∞ -norm. Its metric is defined as $\|\mathbf{u}_1(t) - \mathbf{u}_2(t)\|_{L^\infty}$ for $\mathbf{u}_1(t)$ and $\mathbf{u}_2(t) \in C_0([0, T]; \mathbb{R}^p)$.

Assumption 2: K is a compact subset of $C_0([0, T]; \mathbb{R}^p)$ and it is closed. From the Arzelà-Ascoli theorem (Beattie and Butzmann, 2013), all functions belonging to K are uniformly bounded and there exists a constant B_K such that $\|u_i(t)\|_{L^\infty} \leq B_K$ for all $\mathbf{u}(t) \in K$ and $1 \leq i \leq p$, where $u_i(t)$ is the i^{th} element of $\mathbf{u}(t)$. It is assumed $B_K \geq 1$. In addition, all functions belonging to K are equicontinuous and there exists a continuous modulus of continuity $\phi_K(t) = [\phi_{K,1}(t), \phi_{K,2}(t), \dots, \phi_{K,p}(t)]^\top$ such that for arbitrary $0 \leq t_1 \leq t_2 \leq T$ and all $\mathbf{u}(t) \in K$, it is satisfied that $|u_i(t_1) - u_i(t_2)| \leq \phi_{K,i}(t_2 - t_1)$, thereby $\|\mathbf{u}(t_1) - \mathbf{u}(t_2)\| \leq \|\phi_K(t_2 - t_1)\|$, where $\phi_{K,i}(t) : [0, +\infty) \rightarrow [0, +\infty)$ is monotonic with $\phi_{K,i}(t) \rightarrow 0$ as $t \rightarrow 0$.

Assumption 3: $\Phi = [\Phi_1, \Phi_2, \dots, \Phi_q] : C_0([0, T]; \mathbb{R}^p) \rightarrow C_0([0, t]; \mathbb{R}^q)$ is a causal and uniformly continuous operator. For $\forall t \in [0, T]$, $\Phi[\mathbf{u}(\tau)](t)$ only depends on $\mathbf{u}(\tau)$ over $\tau \in [0, t]$. For $\forall \varepsilon > 0$, there exists a distance $d_\varepsilon > 0$, such that $\|\mathbf{u}_1(t) - \mathbf{u}_2(t)\|_{L^\infty} < d_\varepsilon \Rightarrow \|\Phi[\mathbf{u}_1(\tau)](t) - \Phi[\mathbf{u}_2(\tau)](t)\|_{L^\infty} < \varepsilon$ for $\forall \mathbf{u}_1(t), \mathbf{u}_2(t) \in C_0([0, t]; \mathbb{R}^p)$.

Assumption 4: Since $\Phi : C_0([0, T]; \mathbb{R}^p) \rightarrow C_0([0, t]; \mathbb{R}^q)$ is a causal and uniformly continuous operator and $K \subseteq C_0([0, t]; \mathbb{R}^p)$ is compact, the image set $\Phi(K) \subseteq C_0([0, T]; \mathbb{R}^q)$ of K by Φ is also compact. There exists a constant $B_{\Phi(K)}$ such that all functions belonging to $\Phi(K)$ are bounded by $B_{\Phi(K)}$, that is $\|v_j(t)\|_{L^\infty} \leq B_{\Phi(K)}$ for all $\mathbf{v}(t) = [v_1(t), v_2(t), \dots, v_q(t)]^\top \in \Phi(K)$ and $1 \leq j \leq q$.

Assumption 5: For each element Φ_j of the causal and uniformly continuous operator $\Phi = [\Phi_1, \Phi_2, \dots, \Phi_q]$, $1 \leq j \leq q$, it is assumed that the first-order derivatives of all temporal functions in the image set $\Phi_j \{C_0([0, T]; \mathbb{R}^p)\}$ by Φ_j are bounded by a finite constant D_{Φ_j} .

Assumption 6: Since $\Phi : C_0([0, T]; \mathbb{R}^p) \rightarrow C_0([0, t]; \mathbb{R}^q)$ is a causal and uniformly continuous operator, its j^{th} element Φ_j has a monotonic continuous modulus of continuity $\phi_{\Phi_j}(\cdot) : [0, +\infty) \rightarrow [0, +\infty)$ with $\phi_{\Phi_j}(r) \rightarrow 0$ as

$r \rightarrow 0$, such that $\|\Phi_j[\mathbf{u}_1(\tau)](t) - \Phi_j[\mathbf{u}_2(\tau)](t)\|_{L^\infty} \leq \phi_{\Phi_j}[\|\mathbf{u}_1(t) - \mathbf{u}_2(t)\|_{L^\infty}]$ for $\forall \mathbf{u}_1(t), \mathbf{u}_2(t) \in C_0([0, T]; \mathbb{R}^p)$. $\phi_\Phi(\cdot) = \sum_{j=1}^q \phi_{\Phi_j}(\cdot) : [0, +\infty) \rightarrow [0, +\infty)$ with $\phi_\Phi(r) \rightarrow 0$ as $r \rightarrow 0$, is a monotonic modulus of continuity of Φ , such that $\|\Phi[\mathbf{u}_1(\tau)](t) - \Phi[\mathbf{u}_2(\tau)](t)\|_{L^\infty} \leq \sum_{j=1}^q \|\Phi_j[\mathbf{u}_1(\tau)](t) - \Phi_j[\mathbf{u}_2(\tau)](t)\|_{L^\infty} \leq \phi_\Phi[\|\mathbf{u}_1(t) - \mathbf{u}_2(t)\|_{L^\infty}]$ for $\forall \mathbf{u}_1(t), \mathbf{u}_2(t) \in C_0([0, T]; \mathbb{R}^p)$.

Definition 1 (Hanson and Raginsky, 2020): Given a second-order ODE $\hat{\mathbf{x}}''(t) = g[\hat{\mathbf{x}}(t), \hat{\mathbf{x}}'(t), \mathbf{u}(t)]$ with its state function $\mathbf{z}(t) = [\hat{\mathbf{x}}^\top(t), \hat{\mathbf{x}}'^\top(t)]^\top$, where $\hat{\mathbf{x}}(t) = [\hat{x}_1(t), \hat{x}_2(t), \dots, \hat{x}_r(t)]^\top$, it is uniformly asymptotically incrementally stable for the inputs in a subset $K \subset C_0([0, T]; \mathbb{R}^p)$ on a domain $\Omega_{\mathbf{z}} \subset \mathbb{R}^{2r}$ if there exists a set of non-negative stability functions $\beta_k(h, t)$ over $h \geq 0$ and $t \geq 0$, $k = 1, 2, \dots, 2r$, where $\beta_k(0, t) = 0$, $\lim_{t \rightarrow +\infty} \beta_k(h, t) = 0$, $\beta_k(h, t)$ is continuous and strictly increasing with respect to h and is continuous and strictly decreasing with respect to t , such that $|z_k(t, \mathbf{z}_\tau) - z_k(t, \hat{\mathbf{z}}_\tau)| \leq \beta_k(\|\mathbf{z}_\tau - \hat{\mathbf{z}}_\tau\|_2, t - \tau)$ holds for all $\mathbf{u}(t) \in K$, all \mathbf{z}_τ and $\hat{\mathbf{z}}_\tau \in \Omega_{\mathbf{z}}$, all $t \in [0, T]$, and all $0 \leq \tau \leq t$, where $z_k(t, \mathbf{z}_\tau)$ is the k^{th} element of $\mathbf{z}(t, \mathbf{z}_\tau)$ and $\mathbf{z}(t, \mathbf{z}_\tau)$ represents the solution $\mathbf{z}(t)$ at t driven by $\mathbf{u}(t)$ with an initial condition \mathbf{z}_τ at an initial time instant τ , $0 \leq \tau \leq t$. The corresponding stability bound B_β is calculated as

$$B_\beta = \int_0^{+\infty} \frac{\partial}{\partial h} \sum_{k=1}^{2r} \beta_k(h, \tau) \Big|_{h=0^+} d\tau. \quad (4)$$

Lemma 1 (Theorem 1 of Huang et al. 2025): Given a compact subset $K \subset C_0([0, T]; \mathbb{R}^p)$ and a causal and uniformly continuous operator $\Phi : C_0([0, T]; \mathbb{R}^p) \rightarrow C_0([0, T]; \mathbb{R}^q)$ satisfying Assumptions 1 to 6 with $\phi_K(t) = L_K[t, t, \dots, t]^\top$ and $L_K > 0$, for every integer M_Γ larger than an independent deterministic threshold and every positive integer H_Π , there exist two MLPs $\Gamma(\cdot)$ and $\Pi(\cdot)$ employing $\sigma_{\text{ReLU}}(\cdot)$, such that for $\forall \mathbf{u}(t) \in K$, the corresponding solution $\mathbf{y}(t) = [y_1(t), y_2(t), \dots, y_q(t)]^\top$ from Eq. (1) subject to $\mathbf{u}(t)$ with the initial conditions $\mathbf{x}(0) = \mathbf{x}'(0) = \mathbf{0}$ satisfies

$$|\Phi[\mathbf{u}(\tau)](t) - \mathbf{y}(t)| \leq \varepsilon_{\mathbf{y}} \quad (5)$$

for all $t \in [0, T]$, where

$$\varepsilon_{\mathbf{y}} = \phi_\Phi \left[O \left(\frac{pL_K T}{M_\Gamma^{1/3}} \right) \right] + O \left(\frac{qp^3 M_\Gamma^3}{H_\Pi^{1/[p(M_\Gamma+1)+1]}} \right) \quad (6)$$

and $\phi_\Phi(\cdot)$ is the modulus of continuity of Φ in Assumption 6. $\Gamma(\cdot)$ has one hidden layer and the widths of its input, hidden, and output layers are $w_{\Gamma, \text{in}} = p(2M_\Gamma + 1)$, $w_\Gamma = 2pM_\Gamma$, and $w_{\Gamma, \text{out}} = pM_\Gamma$, respectively. For $\Pi(\cdot)$, the widths of its input, hidden, and output layers are $w_{\Pi, \text{in}} = p(M_\Gamma + 1) + 1$, $w_\Pi = q[(pM_\Gamma + 1) + 4]$, and $w_{\Pi, \text{out}} = q$, respectively, and its depth is $h_\Pi = H_\Pi + 1$.

Lemma 2 (Theorem 2 of Huang et al. 2025): Let K be a compact subset of $C_0([0, T]; \mathbb{R}^p)$, a second-order dynamical system

$$\begin{cases} \hat{\mathbf{x}}''(t) = g[\hat{\mathbf{x}}(t), \hat{\mathbf{x}}'(t), \mathbf{u}(t)] \\ \hat{\mathbf{y}}(t) = h[\hat{\mathbf{x}}(t)] \end{cases}, \quad (7)$$

with $\hat{\mathbf{x}}(0) = \hat{\mathbf{x}}'(0) = \mathbf{0}$, is uniformly asymptotically incrementally stable for all $\mathbf{u}(t) \in K$ on a domain $[-B_{\mathbf{x}}, B_{\mathbf{x}}]^r \times [-B_{\mathbf{x}'}, B_{\mathbf{x}'}]^r \times [-B_K, B_K]^p \subset \mathbb{R}^{2r+p}$, where $\hat{\mathbf{x}}(t) = [\hat{x}_1(t), \hat{x}_2(t), \dots, \hat{x}_r(t)]^\top$, $\hat{\mathbf{y}}(t) = [\hat{y}_1(t), \hat{y}_2(t), \dots, \hat{y}_q(t)]^\top$, $B_{\mathbf{x}} = \alpha B_{\beta_g} + B_{\hat{\mathbf{x}}}$, $B_{\mathbf{x}'} = \alpha B_{\beta_g} + B_{\hat{\mathbf{x}'}}$, α is a positive coefficient, $B_{\hat{\mathbf{x}}}$ and $B_{\hat{\mathbf{x}'}}$ are the bounds of $\hat{\mathbf{x}}(t)$ and $\hat{\mathbf{x}}'(t)$, respectively, B_K is the bound of all $\mathbf{u}(t) \in K$ in Assumption 2, and B_{β_g} is the stability bound of the system calculated by Eq. (4). The functions $g(\cdot) = [g_1(\cdot), g_2(\cdot), \dots, g_r(\cdot)]^\top$ and $h(\cdot) = [h_1(\cdot), h_2(\cdot), \dots, h_q(\cdot)]^\top$ are Lipschitz continuous over \mathbb{R}^{2r+p} and \mathbb{R}^r , respectively, with arbitrary finite-order derivatives. Then, for arbitrary positive errors $\varepsilon_1 \leq \alpha/r$ and ε_2 , there exist two one-hidden-layer MLPs $\Gamma(\cdot)$ and $\Pi(\cdot)$ employing $\sigma_{\text{ReLU}}(\cdot)$, such that for $\forall \mathbf{u}(t) \in K$, the corresponding solutions $\mathbf{y}(t)$ to Eq. (1) and $\hat{\mathbf{y}}(t)$ to Eq. (7) satisfy

$$|\mathbf{y}(t) - \hat{\mathbf{y}}(t)| \leq L_h B_{\beta_g} \sqrt{r} \varepsilon_1 + q \varepsilon_2 \quad (8)$$

for all $t \in [0, T]$, where L_h is the Lipschitz constant of $h(\cdot)$. For $\Gamma(\cdot)$, the widths of its input, hidden, and output layers are $w_{\Gamma, \text{in}} = 2r + p$, $w_\Gamma = 8r[C_\Gamma \varepsilon_1^{-2}]$, and $w_{\Gamma, \text{out}} = r$, respectively. For $\Pi(\cdot)$, the widths of its input, hidden, and output layers are $w_{\Pi, \text{in}} = r + p + 1$, $w_\Pi = 8q[C_\Pi \varepsilon_2^{-2}]$, and $w_{\Pi, \text{out}} = q$, respectively. C_Γ is a constant only depending on $g(\cdot)$, $\sigma_{\text{ReLU}}(\cdot)$, r , p , $B_{\mathbf{x}}$, $B_{\mathbf{x}'}$, and B_K . C_Π is a constant only depending on $h(\cdot)$, $\sigma_{\text{ReLU}}(\cdot)$, r , and B_K .

Remark 1: Lemma 1 proves that the neural oscillator in Eq. (1) can function as a universal approximator of causal and uniformly continuous operators by first encoding an input function $\mathbf{u}(t)$ into the intermediate function $\mathbf{x}(t)$ through the second-order ODE in Eq. (1), and then mapping $\mathbf{x}(t)$, together with the initial value $\mathbf{u}(0)$ of $\mathbf{u}(t)$ and time t , to the output function $\mathbf{y}(t)$. This capability is similar to the universal approximation property of neural operators (Kovachki et al., 2023). Moreover, for the second-order dynamical systems in science and engineering (Strogatz, 2024), Lemma 2 demonstrates that the neural oscillator can directly approximate these systems using its ODE in Eq. (1) with an efficient neural network size.

In the following content of this section, the established theoretical generalization bounds of the neural oscillator in Eq. (1) are presented in an informal manner. The formal statements of the derived theoretical results are presented in Theorems 1 and 2 in Section 3, together with the supporting lemmas required for their proofs.

Informal Statement of Theorem 1: Under Assumptions 1-11 and the conditions in Lemma 1, for the target causal and uniformly continuous operator Φ , with the specified sizes of $\Gamma(\cdot)$ and $\Pi(\cdot)$ in Lemma 1, the generalization error $\ell(\hat{\Pi} \circ \Phi_{\hat{r}})$ in Eq. (13) of a neural oscillator $\hat{\Pi} \circ \Phi_{\hat{r}}$, that is learned by Eq. (12) with N independent and identically distributed (i.i.d.) sample pairs $\mathbf{U}_N(t)$ and $\mathbf{V}_N(t)$ from the probability measure $\mu(\cdot)$ in Assumption 7, is bounded by

$$\ell(\hat{\Pi} \circ \Phi_{\hat{r}}) \leq T\varepsilon_y^2 + \frac{C_1}{\sqrt{N}} \left[C_2 + \sqrt{0.5 \log(2\delta^{-1})} \right] \quad (9)$$

with probability at least $1 - \delta$ for $\forall \delta \in (0, 1)$, where ε_y is in Eq. (6) in Lemma 1, C_1 and C_2 are two constants scaling polynomially with the sizes and parameter values of $\Gamma(\cdot)$ and $\Pi(\cdot)$, and the time length T .

Informal Statement of Theorem 2: Under Assumptions 1-11 and the conditions in Lemma 2, for the target second-order differential system governed by Eq. (7), with the specified sizes of $\Gamma(\cdot)$ and $\Pi(\cdot)$ in Lemma 2, the generalization error $\ell(\hat{\Pi} \circ \Phi_{\hat{r}})$ of $\hat{\Pi} \circ \Phi_{\hat{r}}$, that is learned by Eq. (12) with N i.i.d. sample pairs $\mathbf{U}_N(t)$ and $\mathbf{V}_N(t)$ from the probability measure $\mu(\cdot)$ in Assumption 7, is bounded by

$$\ell(\hat{\Pi} \circ \Phi_{\hat{r}}) \leq 16T \left(\frac{L_h^2 B_{\beta_g}^2 r^2 C_{\Gamma}}{w_{\Gamma} - 8r} + \frac{q^3 C_{\Pi}}{w_{\Pi} - 8q} \right) + \frac{C_1}{\sqrt{N}} \left[C_2 + \sqrt{0.5 \log(2\delta^{-1})} \right] \quad (10)$$

with probability at least $1 - \delta$ for $\forall \delta \in (0, 1)$, where $w_{\Gamma} > 8\alpha^{-2}r^3 C_{\Gamma} + 8r$, $w_{\Pi} > 8q$, C_{Γ} and C_{Π} are the constants specified in Lemma 2, and C_1 and C_2 are two constants scaling polynomially with the sizes and parameter values of $\Gamma(\cdot)$ and $\Pi(\cdot)$, and the time length T .

3. Upper Generalization Bounds of the Neural Oscillator

In this section, corresponding to the results in Lemmas 1 and 2, the PAC upper generalization bounds for the neural oscillator trained with i.i.d. samples are derived using the method based on the Rademacher complexity and the covering number of a candidate neural oscillator class. This method has been applied to derive the upper generalization bounds of MLPs (Bartlett et al., 2017), RNNs (Chen et al., 2020), neural ODEs (Bleistein and Guilloux, 2023; Marion, 2023), and implicit networks (Fung and Berkels, 2024). First, some additional assumptions and necessary definitions on the loss function, covering number, and Rademacher complexity are provided. Then, Lemmas 3 and 4 demonstrate that the Rademacher complexity of the loss function can be bounded by the expected supremum of a sub-Gaussian process. Lemmas 5-10 bound the expected supremum of the sub-Gaussian process using the covering number of a neural oscillator class. Finally, the upper generalization bounds for the neural oscillator in approximating causal and uniformly continuous operators between continuous temporal function spaces and in approximating the uniformly asymptotically incrementally stable second-order dynamical systems are established in Theorems 1 and 2, respectively. The proofs for Theorems 1 and 2 and all lemmas in this section are provided in Appendix A. Furthermore, based on the established generalization bounds, an additional regularization term constraining the Lipschitz constants of $\Gamma(\cdot)$ and $\Pi(\cdot)$ is added into the loss function to enhance the generalization ability of the neural oscillator.

Assumption 7: $\mu(\cdot)$ is a probability measure supported on the compact set $K \subset C_0([0, t]; \mathbb{R}^p)$.

Assumption 8: Suppose that the sizes of $\Gamma(\cdot)$ in Eq. (2) and $\Pi(\cdot)$ in Eq. (3) are specified according to Lemma 1 or Lemma 2, the input layer widths of $\Gamma(\cdot)$ and $\Pi(\cdot)$ are $w_{\Gamma, \text{in}} = 2r + p$ and $w_{\Pi, \text{in}} = r + p + 1$, respectively. The output

layer widths of $\Gamma(\cdot)$ and $\Pi(\cdot)$ are $w_{\Gamma,\text{out}} = r$ and $w_{\Pi,\text{out}} = q$, respectively. The largest hidden layer widths of $\Gamma(\cdot)$ and $\Pi(\cdot)$ are w_Γ and w_Π , respectively, and the depth h_Π of $\Pi(\cdot)$ satisfies $h_\Pi \geq 2$.

Assumption 9: \mathcal{F}_Γ represents a class of MLPs $\Gamma(\cdot)$ whose sizes are specified in Assumption 8. The weight matrices \mathbf{W}_i and vectors \mathbf{b}_i , $i = 1$ and 2 , of $\Gamma(\cdot) \in \mathcal{F}_\Gamma$ are bounded by $|\mathbf{W}_i|_{\infty,\infty} \leq B_\mathbf{W}$ and $|\mathbf{b}_i|_\infty \leq B_\mathbf{b}$. \mathcal{F}_Π represents a class of MLPs $\Pi(\cdot)$ whose sizes are specified in Assumption 8. The weight matrices $\tilde{\mathbf{W}}_j$ and vectors $\tilde{\mathbf{b}}_j$, $j = 1, 2, \dots, h_\Pi$, of $\Pi(\cdot) \in \mathcal{F}_\Pi$ are bounded by $|\tilde{\mathbf{W}}_j|_{\infty,\infty} \leq B_{\tilde{\mathbf{W}}}$ and $|\tilde{\mathbf{b}}_j|_\infty \leq B_{\tilde{\mathbf{b}}}$. The outputs of all $\Pi(\cdot) \in \mathcal{F}_\Pi$ are bounded by $\|\Pi_j(\mathbf{x})\|_{L^\infty} \leq B_\Pi$, $j = 1, 2, \dots, w_{\Pi,\text{out}}$, where $\Pi_j(\mathbf{x})$ is the j^{th} output of $\Pi(\mathbf{x})$. The bounds $B_\mathbf{W}$ and $B_\mathbf{b}$ depend on the size of $\Gamma(\cdot)$ and the bounds $B_{\tilde{\mathbf{W}}}$, $B_{\tilde{\mathbf{b}}}$, and B_Π depend on the size of $\Pi(\cdot)$, ensuring that the results of Lemma 1 or Lemma 2 can be achieved.

Assumption 10: $\mathcal{F}_{\Phi_\Gamma}$ represents a second-order ODE class whose elements Φ_Γ are governed by the first ODE in Eq. (1) with $\Gamma(\cdot) \in \mathcal{F}_\Gamma$. $\mathcal{F}_{\Pi \circ \Phi_\Gamma}$ represents a neural oscillator class whose elements $\Pi \circ \Phi_\Gamma$ are governed by Eq. (1) with $\Gamma(\cdot) \in \mathcal{F}_\Gamma$ and $\Pi(\cdot) \in \mathcal{F}_\Pi$.

Consider the causal continuous operator $\Phi : K \subset C_0([0, T]; \mathbb{R}^p) \rightarrow C_0([0, T]; \mathbb{R}^q)$ in Assumption 3, given N i.i.d. samples $\mathbf{U}_N(t) = [\mathbf{u}_1(t), \mathbf{u}_2(t), \dots, \mathbf{u}_N(t)]$ from the probability measure $\mu(\cdot)$ in Assumption 7, and the corresponding N output function samples $\mathbf{V}_N(t) = [\mathbf{v}_1(t), \mathbf{v}_2(t), \dots, \mathbf{v}_N(t)]$ with $\mathbf{v}_i(t) = \Phi[\mathbf{u}_i(\tau)](t)$, for a neural oscillator $\Pi \circ \Phi_\Gamma \in \mathcal{F}_{\Pi \circ \Phi_\Gamma}$ in Assumption 10, its empirical loss $\hat{\ell}_{\mathbf{U}_N, \mathbf{V}_N}(\Pi \circ \Phi_\Gamma)$ is defined as

$$\hat{\ell}_{\mathbf{U}_N, \mathbf{V}_N}(\Pi \circ \Phi_\Gamma) = \frac{1}{N} \sum_{i=1}^N \|\mathbf{v}_i(t) - \Pi \circ \Phi_\Gamma[\mathbf{u}_i(\tau)](t)\|_{L^2}^2. \quad (11)$$

An estimated neural oscillator $\hat{\Pi} \circ \Phi_{\hat{\Gamma}}$ is learned by the following optimization problem

$$\hat{\Pi} \circ \Phi_{\hat{\Gamma}} \in \arg \min_{\Pi \circ \Phi_\Gamma \in \mathcal{F}_{\Pi \circ \Phi_\Gamma}} \hat{\ell}_{\mathbf{U}_N, \mathbf{V}_N}(\Pi \circ \Phi_\Gamma). \quad (12)$$

An generalization error $\ell(\hat{\Pi} \circ \Phi_{\hat{\Gamma}})$ of $\hat{\Pi} \circ \Phi_{\hat{\Gamma}}$ is calculated as

$$\ell(\hat{\Pi} \circ \Phi_{\hat{\Gamma}}) = \mathbb{E}_{\mathbf{u} \sim \mu} \vartheta_{\hat{\Pi} \circ \Phi_{\hat{\Gamma}}}[\mathbf{u}(\tau)] = \int_K \vartheta_{\hat{\Pi} \circ \Phi_{\hat{\Gamma}}}[\mathbf{u}(\tau)] d\mu[\mathbf{u}(\tau)], \quad (13)$$

where

$$\vartheta_{\hat{\Pi} \circ \Phi_{\hat{\Gamma}}}[\mathbf{u}(\tau)] = \|\Phi[\mathbf{u}(\tau)](t) - \hat{\Pi} \circ \Phi_{\hat{\Gamma}}[\mathbf{u}(\tau)](t)\|_{L^2}^2. \quad (14)$$

Assumption 11: Since the outputs of all neural oscillators in $\mathcal{F}_{\Pi \circ \Phi_\Gamma}$ are bounded by B_Π from Assumptions 9 and 10, and $\mathbf{v}(t) = \Phi[\mathbf{u}(\tau)](t)$ with $\mathbf{u}(t) \in K$ is bounded by $B_{\Phi(K)}$ in Assumption 4, the empirical loss $\hat{\ell}_{\mathbf{U}_N, \mathbf{V}_N}$ and generalization error ℓ are bounded by $\hat{\ell}_{\mathbf{U}_N, \mathbf{V}_N}, \ell \leq TqB_{\text{loss}}^2$, where $B_{\text{loss}} = B_\Pi + B_{\Phi(K)}$.

Definition 2 (Cover): Let \mathcal{M} be a space with a pseudo-metric $d_\mathcal{M}$, for any real $\varepsilon > 0$, a subset $\mathcal{S} \subset \mathcal{M}$ is an ε -cover of \mathcal{M} with respect to $d_\mathcal{M}$ if for $\forall f \in \mathcal{M}$, there exists $\tilde{f} \in \mathcal{S}$, such that $d_\mathcal{M}(f, \tilde{f}) < \varepsilon$.

Definition 3 (Covering number, Definition 2.2.3 of van der Vaart and Wellner 2013): Let \mathcal{M} be a space with a pseudo-metric $d_\mathcal{M}$, for any real $\varepsilon > 0$, the covering number of \mathcal{M} is defined as $N(\mathcal{M}, d_\mathcal{M}, \varepsilon) = \min\{\#\mathcal{S} : \mathcal{S} \text{ is an } \varepsilon\text{-cover of } \mathcal{M}\}$, where $\#\mathcal{S}$ is the cardinality of \mathcal{S} .

Definition 4 (Empirical Rademacher Complexity, Definition 3.1 of Mohri et al. 2018): Given N i.i.d. samples $\mathbf{U}_N(t) = [\mathbf{u}_1(t), \mathbf{u}_2(t), \dots, \mathbf{u}_N(t)]$ from $\mu(\cdot)$ in Assumption 7, the empirical Rademacher complexity $\mathfrak{R}_{\mathcal{G}_\theta}$ of the functional class for $\vartheta_{\Pi \circ \Phi_\Gamma}[\mathbf{u}(\tau)]$ in Eq. (14) with $\Pi \circ \Phi_\Gamma \in \mathcal{F}_{\Pi \circ \Phi_\Gamma}$ is defined as

$$\mathfrak{R}_{\mathcal{G}_\theta} = \mathbb{E}_\sigma \sup_{\Pi \circ \Phi_\Gamma \in \mathcal{F}_{\Pi \circ \Phi_\Gamma}} \frac{1}{N} \sum_{i=1}^N \sigma_i \vartheta_{\Pi \circ \Phi_\Gamma}[\mathbf{u}_i(\tau)], \quad (15)$$

where $\sigma = [\sigma_1, \sigma_2, \dots, \sigma_N]$ is a Rademacher vector of i.i.d. Rademacher variables σ_i taking values of 1 or -1 with equal probability and $i = 1, 2, \dots, N$.

Lemma 3: Given N i.i.d. samples $\mathbf{U}_N(t) = [\mathbf{u}_1(t), \mathbf{u}_2(t), \dots, \mathbf{u}_N(t)]$ from $\mu(\cdot)$ in Assumption 7, the empirical Rademacher complexity $\mathfrak{R}_{\mathcal{G}_\theta}$ in Eq. (15) is bounded by

$$\mathfrak{R}_{\mathcal{G}_\theta} \leq \frac{2\sqrt{2T}w_{\Pi,\text{out}}B_{\text{loss}}}{N} \mathbb{E}_{\tilde{\sigma}} \sup_{\Pi \circ \Phi_\Gamma \in \mathcal{F}_{\Pi \circ \Phi_\Gamma}} \kappa(\Pi \circ \Phi_\Gamma, \tilde{\sigma}), \quad (16)$$

where

$$\kappa(\Pi \circ \Phi_\Gamma, \tilde{\sigma}) = \sum_{i=1}^N \sum_{j=1}^{w_{\Pi, \text{out}}} \sum_{k=1}^{+\infty} \tilde{\sigma}_{ijk} \alpha_{jk} \left\{ \Pi \circ \Phi_\Gamma [\mathbf{u}_i(\tau)]_j \right\}, \quad (17)$$

B_{loss} is in Assumption 11, $\alpha_{jk} \left\{ \Pi \circ \Phi_\Gamma [\mathbf{u}_i(\tau)]_j \right\}$ is the coefficient of $\Pi \circ \Phi_\Gamma [\mathbf{u}_i(\tau)]_j(t)$ under a countable set of standard orthogonal basis functions $e_k(t)$ over $[0, T]$, $i = 1, 2, \dots, N$, $j = 1, 2, \dots, w_{\Pi, \text{out}}$, $k = 1, 2, \dots$, and $\tilde{\sigma}$ is a third-order tensor with elements $\tilde{\sigma}_{ijk}$ being i.i.d. Rademacher variables over discrete indices i, j , and k .

Lemma 4: Under the conditions in Lemma 3, $\kappa(\Pi \circ \Phi_\Gamma, \tilde{\sigma})$ in Eq. (17) is a zero-mean sub-Gaussian process with respect to $\Pi \circ \Phi_\Gamma$ over $\mathcal{F}_{\Pi \circ \Phi_\Gamma}$ satisfying

$$\mathbb{E}_{\tilde{\sigma}} \exp \left\{ w \left[\kappa(\Pi_1 \circ \Phi_{\Gamma_1}, \tilde{\sigma}) - \kappa(\Pi_2 \circ \Phi_{\Gamma_2}, \tilde{\sigma}) \right] \right\} \leq \exp \left\{ 0.5w^2 d_\kappa^2(\Pi_1 \circ \Phi_{\Gamma_1}, \Pi_2 \circ \Phi_{\Gamma_2}) \right\} \quad (18)$$

for $\forall w \in \mathbb{R}$ and $\forall \Pi_1 \circ \Phi_{\Gamma_1}, \forall \Pi_2 \circ \Phi_{\Gamma_2} \in \mathcal{F}_{\Pi \circ \Phi_\Gamma}$, where the pseudo-metric $d_\kappa(\Pi_1 \circ \Phi_{\Gamma_1}, \Pi_2 \circ \Phi_{\Gamma_2})$ is

$$d_\kappa(\Pi_1 \circ \Phi_{\Gamma_1}, \Pi_2 \circ \Phi_{\Gamma_2}) = \sqrt{\sum_{i=1}^N \left\| \Pi_1 \circ \Phi_{\Gamma_1} [\mathbf{u}_i(\tau)](t) - \Pi_2 \circ \Phi_{\Gamma_2} [\mathbf{u}_i(\tau)](t) \right\|_{L_2}^2}. \quad (19)$$

The diameter $\Delta_\kappa(\mathcal{F}_{\Pi \circ \Phi_\Gamma})$ of $\kappa(\Pi \circ \Phi_\Gamma, \tilde{\sigma})$ over $\mathcal{F}_{\Pi \circ \Phi_\Gamma}$ is bounded by

$$\Delta_\kappa(\mathcal{F}_{\Pi \circ \Phi_\Gamma}) = \sup_{\Pi_1 \circ \Phi_{\Gamma_1}, \Pi_2 \circ \Phi_{\Gamma_2} \in \mathcal{F}_{\Pi \circ \Phi_\Gamma}} d_\kappa(\Pi_1 \circ \Phi_{\Gamma_1}, \Pi_2 \circ \Phi_{\Gamma_2}) \leq 2 \sqrt{NT w_{\Pi, \text{out}}} B_\Pi, \quad (20)$$

where B_Π is in Assumption 9.

Given a neural oscillator $\hat{\Pi} \circ \Phi_{\hat{\Gamma}}$ learned from N i.i.d. sample pairs $\mathbf{U}_N(t)$ and $\mathbf{V}_N(t)$ using Eq. (12), from Theorem 11.3 of Mohri et al. (2018), for $\forall \delta \in (0, 1)$, the generalization error $\ell(\hat{\Pi} \circ \Phi_{\hat{\Gamma}})$ of $\hat{\Pi} \circ \Phi_{\hat{\Gamma}}$, which is calculated using Eq. (13), is bounded by

$$\ell(\hat{\Pi} \circ \Phi_{\hat{\Gamma}}) \leq \underbrace{\hat{\ell}_{\mathbf{U}_N, \mathbf{V}_N}(\hat{\Pi} \circ \Phi_{\hat{\Gamma}})}_{\text{approximation error}} + \underbrace{2\mathfrak{R}_{\mathcal{G}_\theta} + 3T w_{\Pi, \text{out}} B_{\text{loss}}^2 \sqrt{\frac{\log(2\delta^{-1})}{2N}}}_{\text{estimation error}} \quad (21)$$

with probability at least $1 - \delta$. In Eq. (21), the empirical loss $\hat{\ell}_{\mathbf{U}_N, \mathbf{V}_N}(\hat{\Pi} \circ \Phi_{\hat{\Gamma}})$ can be bounded using the approximation error bounds in Lemma 1 or Lemma 2. The empirical Rademacher complexity $\mathfrak{R}_{\mathcal{G}_\theta}$ can be bounded by the expected supremum of the sub-Gaussian process $\kappa(\Pi \circ \Phi_\Gamma, \tilde{\sigma})$, as demonstrated in Lemma 3. Based on the Dudley entropy integral bound (Theorem 8.23 of Foucart and Rauhut, 2013), the expected supremum of $\kappa(\Pi \circ \Phi_\Gamma, \tilde{\sigma})$ over $\mathcal{F}_{\Pi \circ \Phi_\Gamma}$ can be bounded by the covering number $N(\mathcal{F}_{\Pi \circ \Phi_\Gamma}, d_\kappa, \varepsilon)$ of $\mathcal{F}_{\Pi \circ \Phi_\Gamma}$

$$\mathbb{E}_{\tilde{\sigma}} \sup_{\Pi \circ \Phi_\Gamma \in \mathcal{F}_{\Pi \circ \Phi_\Gamma}} \kappa(\Pi \circ \Phi_\Gamma, \tilde{\sigma}) \leq 4\sqrt{2} \int_0^{\sqrt{NT w_{\Pi, \text{out}}} B_\Pi} \sqrt{\ln N(\mathcal{F}_{\Pi \circ \Phi_\Gamma}, d_\kappa, \varepsilon)} d\varepsilon. \quad (22)$$

For the sake of completeness, the proof of Eq. (22) is provided in Appendix B.

In what follows, the bound of the covering number $N(\mathcal{F}_{\Pi \circ \Phi_\Gamma}, d_\kappa, \varepsilon)$ is derived. Subsequently, the bound of the expected supremum of $\kappa(\Pi \circ \Phi_\Gamma, \tilde{\sigma})$ is obtained using the bound of $N(\mathcal{F}_{\Pi \circ \Phi_\Gamma}, d_\kappa, \varepsilon)$. Finally, by substituting the bound of the expected supremum of $\kappa(\Pi \circ \Phi_\Gamma, \tilde{\sigma})$ into Eq. (16) in Lemma 3, the bound of the generalization error $\ell(\hat{\Pi} \circ \Phi_{\hat{\Gamma}})$ can be derived using Eq. (21).

Lemma 5: Under Assumptions 8 and 9, all $\Gamma(\cdot) \in \mathcal{F}_\Gamma$ and $\Pi(\cdot) \in \mathcal{F}_\Pi$ are Lipschitz continuous. $L_{\mathcal{F}_\Gamma} = w_{\Gamma, \text{out}} w_\Gamma B_{\mathbf{W}}^2$ is an L^1 -norm Lipschitz constant of all $\Gamma(\cdot) \in \mathcal{F}_\Gamma$. $L_{\mathcal{F}_\Pi} = w_{\Pi, \text{out}} w_\Pi^{h_\Pi - 1} B_{\mathbf{W}}^{h_\Pi}$ is an L^1 -norm Lipschitz constant of all $\Pi(\cdot) \in \mathcal{F}_\Pi$.

Lemma 6: Under Assumptions 2, 8, 9, and 10, for all $\Phi_\Gamma \in \mathcal{F}_{\Phi_\Gamma}$ and all $\mathbf{u}(t) \in K$, $\mathbf{x}(t) = \Phi_\Gamma[\mathbf{u}(\tau)](t)$ with the initial conditions $\mathbf{x}(0) = \mathbf{x}'(0) = \mathbf{0}$ satisfies

$$\max_{t \in [0, T]} \left[|\mathbf{x}(t)| + |\mathbf{x}'(t)| \right] \leq T \left[p B_K L_{\mathcal{F}_\Gamma} + w_{\Gamma, \text{out}} B_{\mathbf{b}} (w_\Gamma B_{\mathbf{W}} + 1) \right] e^{T(L_{\mathcal{F}_\Gamma} + 1)}, \quad (23)$$

where $L_{\mathcal{F}_T}$ is an arbitrary L^1 -norm Lipschitz constant for all $\Gamma(\cdot) \in \mathcal{F}_T$.

Lemma 7: Under Assumptions 1, 2, 8, 9, and 10, given MLPs $\Gamma_1(\cdot)$ and $\Gamma_2(\cdot) \in \mathcal{F}_T$, the differences between their weight matrices and vectors are bounded by ς , that is $|\mathbf{W}_{2,i} - \mathbf{W}_{1,i}|_{\infty, \infty} \leq \varsigma$ and $|\mathbf{b}_{2,i} - \mathbf{b}_{1,i}|_{\infty} \leq \varsigma$, where $\mathbf{W}_{j,i}$ and $\mathbf{b}_{j,i}$ are respectively the weight matrix and vector of $\Gamma_j(\cdot)$, and $i, j = 1$ and 2 , then, for all $\mathbf{u}(t) \in K$, the difference between $\mathbf{x}_1(t) = \Phi_{\Gamma_1}[\mathbf{u}(\tau)](t)$ and $\mathbf{x}_2(t) = \Phi_{\Gamma_2}[\mathbf{u}(\tau)](t)$, with the initial conditions $\mathbf{x}_1(0) = \mathbf{x}'_1(0) = \mathbf{x}_2(0) = \mathbf{x}'_2(0) = \mathbf{0}$, is bounded by

$$\max_{t \in [0, T]} |\mathbf{x}_2(t) - \mathbf{x}_1(t)| \leq 2\varsigma w_{\Gamma, \text{out}} w_{\Gamma} p T^2 e^{2T(L_{\mathcal{F}_T} + 1)} \{ \max(B_{\mathbf{W}}, B_{\mathbf{b}}) [B_K (L_{\mathcal{F}_T} + 1) + w_{\Gamma, \text{out}} B_{\mathbf{b}} (w_{\Gamma} B_{\mathbf{W}} + 1) + 1] + 1 \}, \quad (24)$$

where $L_{\mathcal{F}_T}$ is an arbitrary L^1 -norm Lipschitz constant for all $\Gamma(\cdot) \in \mathcal{F}_T$.

Lemma 8: Under Assumptions 8 and 9, given MLPs $\Pi_1(\cdot)$ and $\Pi_2(\cdot) \in \mathcal{F}_{\Pi}$, the differences between their weight matrices and vectors are bounded by ς , that is $|\tilde{\mathbf{W}}_{2,i} - \tilde{\mathbf{W}}_{1,i}|_{\infty, \infty} \leq \varsigma$ and $|\tilde{\mathbf{b}}_{2,i} - \tilde{\mathbf{b}}_{1,i}|_{\infty} \leq \varsigma$, where $\tilde{\mathbf{W}}_{j,i}$ and $\tilde{\mathbf{b}}_{j,i}$ are respectively the weight matrix and vector of $\Pi_j(\cdot)$, $i = 1, 2, \dots, h_{\Pi}$ and $j = 1$ and 2 , then $|\Pi_1(\mathbf{x}) - \Pi_2(\mathbf{x})|$ is bounded by

$$|\Pi_1(\mathbf{x}) - \Pi_2(\mathbf{x})| \leq \varsigma \max(w_{\Gamma, \text{out}}, w_{\Gamma}) h_{\Pi}^2 \left(L_{\mathcal{F}_{\Pi, \text{layer}}}^{h_{\Pi} - 1} + 1 \right) (|\mathbf{x}| + w_{\Pi} B_{\tilde{\mathbf{b}}} + 1), \quad (25)$$

where $L_{\mathcal{F}_{\Pi, \text{layer}}}$ is an arbitrary L^1 -norm Lipschitz constant that simultaneously bounds the mappings between all adjacent layers of all $\Pi(\cdot) \in \mathcal{F}_{\Pi}$.

Lemma 9: Under Assumptions 1, 2, 8, 9, and 10, given MLPs $\Gamma_1(\cdot)$ and $\Gamma_2(\cdot) \in \mathcal{F}_T$ and MLPs $\Pi_1(\cdot)$ and $\Pi_2(\cdot) \in \mathcal{F}_{\Pi}$, the differences between the weight matrices and vectors of $\Gamma_1(\cdot)$ and $\Gamma_2(\cdot)$ and those of $\Pi_1(\cdot)$ and $\Pi_2(\cdot)$ are bounded by ς , as specified in Lemmas 7 and 8, then, for all $\mathbf{u}(t) \in K$, the difference between $\Pi_1 \circ \Phi_{\Gamma_1}[\mathbf{u}(\tau)](t)$ and $\Pi_2 \circ \Phi_{\Gamma_2}[\mathbf{u}(\tau)](t)$, with the initial conditions $\mathbf{x}_1(0) = \mathbf{x}'_1(0) = \mathbf{x}_2(0) = \mathbf{x}'_2(0) = \mathbf{0}$, is bounded by

$$\max_{t \in [0, T]} |\Pi_1 \circ \Phi_{\Gamma_1}[\mathbf{u}(\tau)](t) - \Pi_2 \circ \Phi_{\Gamma_2}[\mathbf{u}(\tau)](t)| \leq 3\varsigma \left(L_{\mathcal{F}_{\Pi, \text{layer}}}^{h_{\Pi}} + 1 \right) w_{\Pi} w_{\Gamma, \text{out}}^2 w_{\Gamma}^2 h_{\Pi}^2 p T^2 e^{2T(L_{\mathcal{F}_T} + 1)} (L_{\mathcal{F}_T} + 1) B_K B(B_{\tilde{\mathbf{W}}}, B_{\tilde{\mathbf{b}}}, B_{\mathbf{W}}, B_{\mathbf{b}}), \quad (26)$$

where $L_{\mathcal{F}_T}$ is an arbitrary L^1 -norm Lipschitz constant for all $\Gamma(\cdot) \in \mathcal{F}_T$, $L_{\mathcal{F}_{\Pi, \text{layer}}}$ is an arbitrary inter-layer L^1 -norm Lipschitz constant for all $\Pi(\cdot) \in \mathcal{F}_{\Pi}$, and

$$B(B_{\tilde{\mathbf{W}}}, B_{\tilde{\mathbf{b}}}, B_{\mathbf{W}}, B_{\mathbf{b}}) = [\max(B_{\mathbf{W}}, B_{\mathbf{b}}) + 1] [B_{\tilde{\mathbf{b}}} (B_{\mathbf{W}} + 1) + 2] + B_{\tilde{\mathbf{b}}} + 2. \quad (27)$$

Lemma 10: Under Assumptions 1, 2, 8, 9, and 10, the expected supremum of $\kappa(\Pi \circ \Phi_{\Gamma}, \tilde{\sigma})$ in Eq. (22) can be bounded by

$$\mathbb{E}_{\tilde{\sigma}} \sup_{\Pi \circ \Phi_{\Gamma} \in \mathcal{F}_{\Pi \circ \Phi_{\Gamma}}} \kappa(\Pi \circ \Phi_{\Gamma}, \tilde{\sigma}) \leq 32 \sqrt{2} B_{\Pi} w_{\max}^{1.5} h_{\Pi} \sqrt{NT \ln(3 + 6B_{\max} \Delta_{\Pi \circ \Phi_{\Gamma}})}, \quad (28)$$

where

$$\Delta_{\Pi \circ \Phi_{\Gamma}} = 30 w_{\max}^{5.5} h_{\Pi}^2 \left(L_{\mathcal{F}_{\Pi, \text{layer}}}^{h_{\Pi}} + 1 \right) (L_{\mathcal{F}_T} + 1) T^2 e^{2T(L_{\mathcal{F}_T} + 1)} B_{\Pi}^{-1} B_K (B_{\max}^3 + 1), \quad (29)$$

$w_{\max} = \max(w_{\Pi, \text{in}}, w_{\Pi}, w_{\Pi, \text{out}}, w_{\Gamma, \text{in}}, w_{\Gamma}, w_{\Gamma, \text{out}})$, $B_{\max} = \max(B_{\mathbf{W}}, B_{\mathbf{b}}, B_{\tilde{\mathbf{W}}}, B_{\tilde{\mathbf{b}}})$, $L_{\mathcal{F}_T}$ is an arbitrary L^1 -norm Lipschitz constant for all $\Gamma(\cdot) \in \mathcal{F}_T$, and $L_{\mathcal{F}_{\Pi, \text{layer}}}$ is an arbitrary inter-layer L^1 -norm Lipschitz constant for all $\Pi(\cdot) \in \mathcal{F}_{\Pi}$.

Theorem 1: Under Assumptions 1-11 and the conditions in Lemma 1, for the target causal and uniformly continuous operator Φ , with the specified sizes of $\Gamma(\cdot)$ and $\Pi(\cdot)$ in Lemma 1, the generalization error $\ell(\hat{\Pi} \circ \Phi_{\hat{r}})$ of a neural oscillator $\hat{\Pi} \circ \Phi_{\hat{r}}$, that is learned by Eq. (12) with N i.i.d. sample pairs $\mathbf{U}_N(t)$ and $\mathbf{V}_N(t)$ from $\mu(\cdot)$, is bounded by

$$\ell(\hat{\Pi} \circ \Phi_{\hat{r}}) \leq T \varepsilon_{\mathbf{y}}^2 + 3 \frac{T q B_{\text{loss}}^2}{\sqrt{N}} \left[86 w_{\max}^{1.5} h_{\Pi} \sqrt{\ln(3 + 6B_{\max} \Delta_{\Pi \circ \Phi_{\Gamma}})} + \sqrt{0.5 \log(2\delta^{-1})} \right] \quad (30)$$

with probability at least $1 - \delta$ for $\forall \delta \in (0, 1)$, where $\varepsilon_{\mathbf{y}}$ is in Eq. (6) in Lemma 1, $\Delta_{\Pi \circ \Phi_{\Gamma}}$ is in Eq. (29) with $L_{\mathcal{F}_T} = w_{\max}^2 B_{\max}^2$, $L_{\mathcal{F}_{\Pi, \text{layer}}}^{h_{\Pi}} = w_{\max}^{h_{\Pi}} B_{\max}^{h_{\Pi}}$, and $w_{\Pi, \text{out}} = q$.

Theorem 2: Under Assumptions 1-11 and the conditions in Lemma 2, for the target second-order differential system governed by Eq. (7), with the specified sizes of $\Gamma(\cdot)$ and $\Pi(\cdot)$ in Lemma 2, the generalization error $\ell(\hat{\Pi} \circ \Phi_{\hat{r}})$ of $\hat{\Pi} \circ \Phi_{\hat{r}}$, that is learned by Eq. (12) with N i.i.d. sample pairs $\mathbf{U}_N(t)$ and $\mathbf{V}_N(t)$ from $\mu(\cdot)$, is bounded by

$$\ell(\hat{\Pi} \circ \Phi_{\hat{r}}) \leq 16T \left(\frac{L_h^2 B_{\beta_s}^2 r^2 C_{\Gamma}}{w_{\Gamma} - 8r} + \frac{q^3 C_{\Pi}}{w_{\Pi} - 8q} \right) + 3 \frac{T q B_{\text{loss}}^2}{\sqrt{N}} \left[172 w_{\max}^{1.5} \sqrt{\ln(3 + 6B_{\max} \Delta_{\Pi \circ \Phi_{\Gamma}})} + \sqrt{0.5 \log(2\delta^{-1})} \right] \quad (31)$$

with probability at least $1 - \delta$ for $\forall \delta \in (0, 1)$, where $w_\Gamma > 8\alpha^{-2}r^3C_\Gamma + 8r$, $w_\Pi > 8q$, $\Delta_{\Pi \circ \Phi_\Gamma}$ is in Eq. (29) with $h_\Pi = 2$, $w_{\Gamma, \text{out}} = r$, $L_{\mathcal{F}_\Gamma} = w_{\max}^2 B_{\max}^2$, $L_{\mathcal{F}_{\Pi, \text{layer}}}^{h_\Pi} = w_{\max}^2 B_{\max}^2$, and $w_{\Pi, \text{out}} = q$, and the constants C_Γ and C_Π are specified in Lemma 2.

Remark 2: An upper generalization bound for a deep SS model has been derived by leveraging the Rademacher complexity combined with a layer-by-layer Rademacher contraction approach (Rácz et al., 2024). The considered deep SS model produces a scalar output through pooling and its derived estimation error grows exponentially with the depth of a utilized MLP. In this study, the outputs of the neural oscillator are continuous temporal functions. The exponential terms in $\Delta_{\Pi \circ \Phi_\Gamma}$ of Eq. (29), which contain the MLP sizes, parameter bound B_{\max} , and time length T , are encapsulated within the logarithmic functions in Eqs. (30) and (31). Consequently, the estimation errors of the generalization bounds established in Theorems 1 and 2 grow polynomially with the sizes and parameter values of the employed MLPs $\Gamma(\cdot)$ and $\Pi(\cdot)$, as well as the time length T . In the numerical study conducted by Huang et al. (2025), the numerical generalization errors can clearly illustrate the decaying approximation error curves of the neural oscillator with the increasing MLP sizes. These results indicate that increasing the MLP sizes has only a marginal influence on the generalization errors, which is consistent with the theoretical results in Theorems 1 and 2 of this study.

Remark 3: Lanthaler (2024) has proved that decreasing the required number of parameters in neural operators using super-expressive neural networks, which aims to mitigate the curse of parametric complexity, may come at the expense of requiring larger model parameter values. The generalization bounds in Theorems 1 and 2 increase with the growing bound B_{\max} of the MLP parameters. Therefore, whether employing super-expressive neural networks can finally decrease the generalization error of the neural oscillator remains an open question. Theorem 10. 4 in Foucart and Rauhut (2013) proves that the Gelfand widths of the normed spaces containing a target operator can be employed to establish lower generalization bounds for all models that approximate this target operator. This method has been employed to prove that polynomial-based neural operators attain the optimal rate of sample complexity for the approximation of Lipschitz operators (Adcock et al., 2025). Utilizing this method to derive lower generalization bounds for the neural oscillator represents an interesting direction for future research.

The estimation errors in Theorems 1 and 2 can be expressed in the form of $N^{-0.5} O \left\{ \left[L_{\mathcal{F}_\Gamma} + \ln(L_{\mathcal{F}_\Gamma}) + h_\Pi \ln(L_{\mathcal{F}_{\Pi, \text{layer}}}) \right]^{0.5} \right\}$, which can be interpreted from a sample-dependent perspective (Wei and Ma, 2019). During a practical training process, each tunable parameter in the matrices and vectors of $\Gamma(\cdot)$ and $\Pi(\cdot)$ varies within a bounded range and attains a largest absolute value. Thus, for each pair of $\Gamma(\cdot)$ and $\Pi(\cdot)$ learned from $\hat{\ell}_{U_N, V_N}(\Pi \circ \Phi_\Gamma)$ in Eq. (12), the MLP spaces \mathcal{F}_Γ and \mathcal{F}_{Π} in Assumption 9 can be narrowed to the ones determined by the largest absolute values of all tunable MLP parameters during the training process, under which all above theoretical results remain valid. In this setting, $L_{\mathcal{F}_\Gamma}$ and $L_{\mathcal{F}_{\Pi, \text{layer}}}$ are the L^1 -norm Lipschitz constants of these two narrowed MLP spaces and they can be much smaller than $w_{\Gamma, \text{out}} w_\Gamma B_{\mathbf{W}}^2$ and $\max(w_{\Pi, \text{out}}, w_\Pi) B_{\mathbf{W}}$, respectively. Therefore, constraining the Lipschitz constants of $\Gamma(\cdot)$ and $\Pi(\cdot)$ rather than the maximum parameter bound B_{\max} provides an effective approach to reducing the generalization error of a neural oscillator learned from samples. Motivated by this observation, a loss function containing explicit constraints on the Lipschitz constants of $\Gamma(\cdot)$ and $\Pi(\cdot)$ is introduced

$$\tilde{\ell}_{U_N, V_N}(\Pi \circ \Phi_\Gamma) = \frac{1}{N} \sum_{i=1}^N \|\mathbf{v}_i(t) - \Pi \circ \Phi_\Gamma[\mathbf{u}_i(\tau)](t)\|_{L^2}^2 + \frac{\lambda_L}{\sqrt{N}} (L_\Gamma + h_\Pi L_{\Pi, \text{layer}}), \quad (32)$$

where λ_L a manually determined parameter, L_Γ is the L^1 -norm Lipschitz constant of $\Gamma(\cdot)$, and $L_{\Pi, \text{layer}}$ is the inter-layer L^1 -norm Lipschitz constant of $\Pi(\cdot)$. Existing methods for constraining Lipschitz constants of MLPs, including weight matrix norm regularization methods (Yoshida and Miyato, 2017), weight matrix normalization methods (Gouk et al., 2021; Liu et al., 2022), and Jacobian regularization methods (Hoffman et al., 2019; Wei and Ma, 2019), can be directly employed to constrain L_Γ and $L_{\Pi, \text{layer}}$. Since the ReLU MLPs $\Gamma(\cdot)$ and $\Pi(\cdot)$ are piecewise affine functions (Hanin, 2019), decreasing the number of affine segments can reduce the Lipschitz constants of $\Gamma(\cdot)$ and $\Pi(\cdot)$ learned from samples. In this study, L_Γ and $h_\Pi L_{\Pi, \text{layer}}$ are respectively replaced by $\sum_{i=1}^2 (|\mathbf{W}_{i1,1}| + |\mathbf{b}_i|_1)$ and $\sum_{j=1}^{h_\Pi} (|\tilde{\mathbf{W}}_j|_{1,1} + |\tilde{\mathbf{b}}_j|_1)$ to enhance the sparsity of $\Gamma(\cdot)$ and $\Pi(\cdot)$, thereby reducing their Lipschitz constants.

4. Numerical Study

In this section, a Bouc-Wen nonlinear system subjected to stochastic seismic excitation, which exhibits plastic deformation responses (Huang et al., 2025), is employed to validate the power laws of the estimation errors in the generalization bounds with respect to the sample size N and time length T , and to demonstrate the effectiveness of $\hat{\ell}_{\mathbf{U}_N, \mathbf{V}_N}$ in Eq. (32) for improving the generalization capability of the neural oscillator under limited training samples. The differential equation of the five-degree of freedom Bouc-Wen system is

$$\begin{cases} \mathbf{M}\ddot{\mathbf{X}}(t) + \mathbf{C}\dot{\mathbf{X}}(t) + \lambda\mathbf{K}\mathbf{X}(t) + (1 - \lambda)\tilde{\mathbf{K}}\mathbf{Z}(t) = -\mathbf{M}U_e(t) \\ \dot{Z}_i(t) = \dot{X}_i(t) - \beta \left| \dot{X}_i(t) \right| |Z_i(t)|^{s-1} Z_i(t) - \gamma \dot{X}_i(t) |Z_i(t)|^s, \quad i = 1, 2, \dots, 5 \end{cases} \quad (33)$$

where $\mathbf{X} = [X_1(t), X_2(t), \dots, X_5(t)]^\top$, $\tilde{\mathbf{X}}(t) = [X_1(t), X_2(t) - X_1(t), X_3(t) - X_2(t), \dots, X_5(t) - X_4(t)]^\top$, $\mathbf{Z} = [Z_1(t), Z_2(t), \dots, Z_5(t)]^\top$, $\mathbf{X}(0) = \mathbf{X}'(0) = \mathbf{Z}(0) = \mathbf{0}$,

$$\mathbf{M} = \begin{bmatrix} m & 0 & 0 & 0 & 0 \\ 0 & m & 0 & 0 & 0 \\ 0 & 0 & m & 0 & 0 \\ 0 & 0 & 0 & m & 0 \\ 0 & 0 & 0 & 0 & m \end{bmatrix}, \quad \mathbf{K} = \begin{bmatrix} 2k & -k & 0 & 0 & 0 \\ -k & 2k & -k & 0 & 0 \\ 0 & -k & 2k & -k & 0 \\ 0 & 0 & -k & 2k & -k \\ 0 & 0 & 0 & -k & k \end{bmatrix}, \quad \tilde{\mathbf{K}} = \begin{bmatrix} k & -k & 0 & 0 & 0 \\ 0 & k & -k & 0 & 0 \\ 0 & 0 & k & -k & 0 \\ 0 & 0 & 0 & k & -k \\ 0 & 0 & 0 & 0 & k \end{bmatrix}, \quad (34)$$

$m = 1382.4$ kilogram, $k = 1.7 \times 10^6$ Newton/meter, \mathbf{C} is determined using \mathbf{M} and \mathbf{K} such that the damping ratios of all response modes are 0.05, $\lambda = 0.01$, $\beta = 2$, $\gamma = 2$, and $s = 3$, and $U_e(t)$ is a stochastic Gaussian harmonizable earthquake ground motion acceleration whose Wigner-ville spectrum is

$$W_e(t, f) = 2500t^2 f^2 \exp[-0.3(1 + f^2)t]. \quad (35)$$

The ODE system in Eq. (33) is solved numerically using a fourth-order Runge-Kutta method (Griffiths and Higham, 2010) with a time discretization of $\Delta t = 0.01$ seconds. For the numerical implementation of training, the neural oscillator is discretized using a second-order Runge-Kutta scheme. The approach for training the neural oscillator with input-output pair samples is briefly described in Appendix C. All code for this numerical study is available at: <https://github.com/ZifengH22/Upper-Generalization-Bounds-for-Neural-Oscillators>.

In this numerical study, the mapping from $U_e(t)$ to the response $X_5(t)$ and that from $U_e(t)$ to the extreme value process $E_{X_5}(t) = \max_{\tau \in [0, t]} |X_5(\tau)|$ of $X_5(t)$ are learned using the neural oscillator with simulated sample pairs. For learning the mapping from $U_e(t)$ to $X_5(t)$, 5×10^4 independent discrete-time samples $U_{e,l}(t_i)$ of $U_e(t)$ over a time interval $[0, 10]$ are simulated, where $i = 0, 1, 2, \dots, 999$ and $l = 1, 2, \dots, 5 \times 10^4$. Their induced 5×10^4 samples $X_{5,l}(t_i)$ of $X_5(t)$ are computed by numerically solving the ODE in Eq. (33). $\Gamma(\cdot)$ and $\Pi(\cdot)$ in Eq. (1) are one-hidden layer MLPs. Their activation functions are $\sigma_{\text{ReLU}}(\cdot)$. The widths of input, hidden, and output layers of $\Gamma(\cdot)$ are 21, 40, and 10, respectively. The widths of input, hidden, and output layers of $\Pi(\cdot)$ are 15, 20, and 10, respectively. Six sets of randomly selected training and validation samples are employed to train the neural oscillator with the loss function $\hat{\ell}_{\lambda_L}$ in Eq. (C.3), both with ($\lambda_L = 0.003$) and without ($\lambda_L = 0$) the parameter-norm constraint. The six datasets respectively contain (i) 100 training and 20 validation samples, (ii) 200 training and 50 validation samples, (iii) 400 training and 100 validation samples, (iv) 800 training and 200 validation samples, (v) 1600 training and 400 validation samples, and (vi) 3200 training and 800 validation samples. All training phases consist of 1000 epochs, each containing 32 batches with a batch size of 100. For each training phase of the six datasets, the initial learning rate is set to 0.01, with a decay period of 100 epochs and a decay factor of 0.965. A gradient-norm clipping strategy (Pascanu et al., 2013) with a threshold of 1 is applied to all MLPs to prevent gradient explosion. $\Gamma(\cdot)$ and $\Pi(\cdot)$ are initialized using identical random seeds to ensure consistent initialization across experiments. The neural oscillator network achieving the smallest training loss is selected as the final model.

For each of all trained neural oscillators using one of the six datasets, its 5×10^4 prediction samples $\tilde{X}_{5,l}(t_i)$ driven by the input samples $U_{e,l}(t_i)$ are simulated. The relative generalization error $\tilde{\epsilon}_{X,2}$ is computed as

$$\tilde{\epsilon}_{X,2} = \frac{\sum_{l=1}^{50000} \sum_{i=0}^{999} [X_{5,l}(t_i) - \tilde{X}_{5,l}(t_i)]^2}{\sum_{l=1}^{50000} \sum_{i=0}^{999} X_{5,l}^2(t_i)}. \quad (36)$$

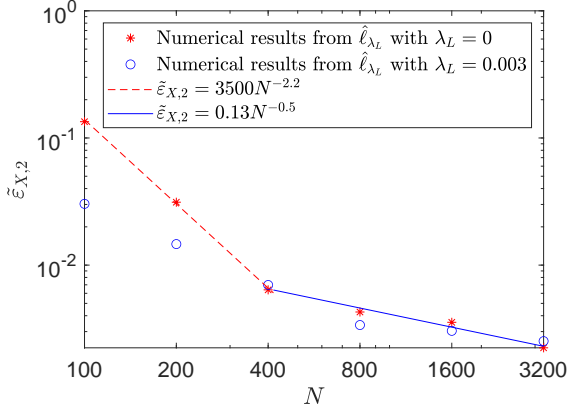


Figure 1: $\tilde{\varepsilon}_{X,2}$ versus N .

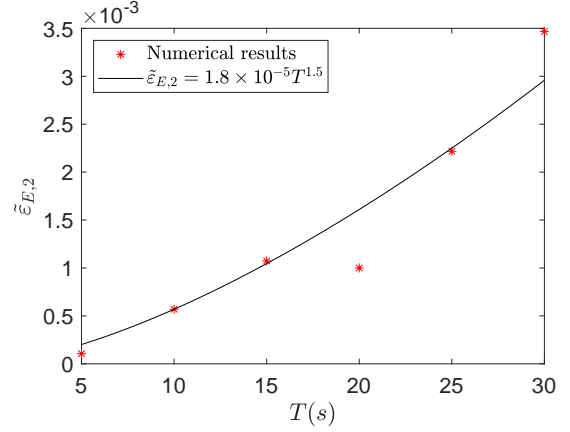


Figure 2: $\tilde{\varepsilon}_{E,2}$ versus T .

The decays of $\tilde{\varepsilon}_{X,2}$ with respect to the increasing sample number N are shown in Figure 1. It can be observed that, for small sample sizes ($N \in [100, 400]$), the decay rate of -2.2 obtained from the numerical results is steeper than the theoretical value of -0.5 in Theorems 1 and 2. As the sample number increases ($N \in [400, 3200]$), the decay rate of the numerical errors coincides with the theoretical value of -0.5 . Since the established theoretical results provide upper generalization bounds, the numerical results in Figure 1 confirm the validity of the decay rate of -0.5 . For small sample sizes ($N \in [100, 200]$), the numerical generalization errors are significantly reduced by constraining the L^1 -norms of the matrices and vectors of $\Gamma(\cdot)$ and $\Pi(\cdot)$ during training. This validates the effectiveness of $\tilde{\ell}_{U_N, V_N}$ in Eq. (32) for decreasing the generalization error of the neural oscillator when training data are limited.

For learning the mapping from $U_e(t)$ to $E_{X_5}(t)$, 5×10^4 independent discrete-time samples $U_{e,l}(t_i)$ of $U_e(t)$ over a time interval $[0, 30]$, where $i = 0, 1, 2, \dots, 2999$ and $l = 1, 2, \dots, 5 \times 10^4$, are simulated. Their induced 5×10^4 samples $E_{X_5,l}(t_i)$ of $E_{X_5}(t)$ are computed by $E_{X_5,l}(t_i) = \max_{\tau \in [0, t_i]} |X_{5,l}(\tau)|$, where $X_{5,l}(t_i)$ is the sample of $X_5(t)$ computed by numerically solving the ODE in Eq. (33). $\Gamma(\cdot)$ in Eq. (1) is a one-hidden layer MLP. The widths of input, hidden, and output layers of $\Gamma(\cdot)$ is 11, 20, and 10, respectively. For $\Pi(\cdot)$, its input, hidden, and output layer widths are 12, 15, and 1, respectively, and its hidden layer number is 2. The activation functions of $\Gamma(\cdot)$ and $\Pi(\cdot)$ adopt the Parametric Rectified Linear Unit (PReLU) $\sigma_{\text{PReLU}}(x) = \max(0, x) + \alpha \min(0, x)$ to facilitate the training process, where α is a parameter learned during training (He et al., 2015). Since $\sigma_{\text{PReLU}}(\cdot)$ is also a piecewise linear activation function with bounded first-order derivatives, the estimation errors in Theorems 1 and 2 remain valid up to a constant factor. Six sets of randomly selected training and validation samples are employed to train the neural oscillator with the loss function $\hat{\ell}_{\lambda_L}$ in Eq. (C.3) without the parameter-norm constraint ($\lambda_L = 0$). Each of the six datasets contains 1600 training and 400 validation samples. The time lengths of the six datasets are 5 seconds, 10 seconds, 15 seconds, 20 seconds, 25 seconds, and 30 seconds, respectively. All training phases consist of 3000 epochs, each containing 16 batches with a batch size of 100. For each training phase of the six datasets, the learning rate first linearly increases from 0.0005 to 0.02 within the first 40 epoches, and subsequently decreases exponentially with a decay period of 100 epochs and a decay factor of 0.95. A gradient-norm clipping strategy (Pascanu et al., 2013) with a threshold of 1 is applied to all MLPs to prevent gradient explosion. $\Gamma(\cdot)$ and $\Pi(\cdot)$ are initialized using identical random seeds to ensure consistent initialization across experiments. The neural oscillator network achieving the smallest training loss is selected as the final model.

For each of all trained neural oscillators using one of the six datasets, its 5×10^4 prediction samples $\tilde{E}_{X_5,l}(t_i)$ driven by the input samples $U_{e,l}(t_i)$ are simulated. The relative generalization error $\tilde{\varepsilon}_{E,2}$ is computed as

$$\tilde{\varepsilon}_{E,2} = \frac{\sum_{l=1}^{50000} \sum_{i=0}^{100T-1} [E_{X_5,l}(t_i) - \tilde{E}_{X_5,l}(t_i)]^2}{\sum_{l=1}^{50000} \sum_{i=0}^{2999} E_{X_5,l}^2(t_i)}. \quad (37)$$

As illustrated in Figure 2, the variation of $\tilde{\varepsilon}_{E,2}$ with respect to the increasing time length T can be approximated by

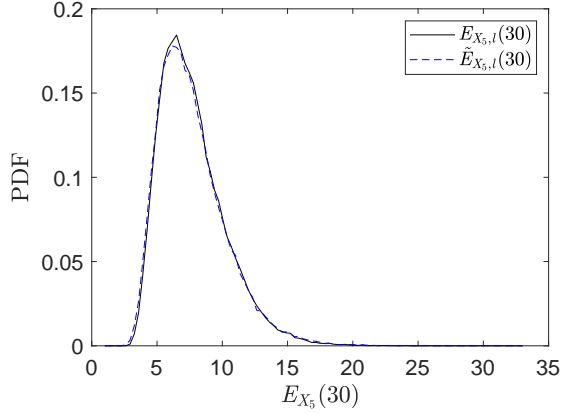


Figure 3: PDF of $E_{X_5}(30)$.

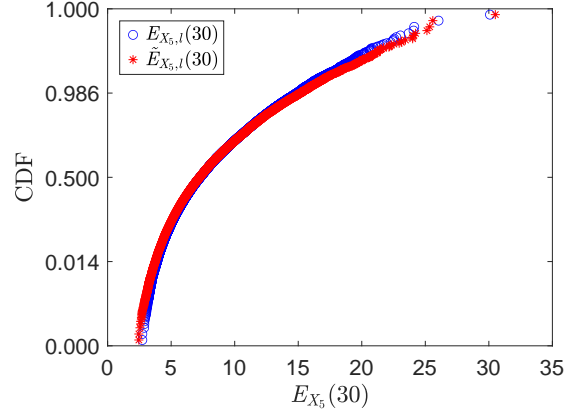


Figure 4: CDF of $E_{X_5}(30)$.

a power-law function with an exponent of 1.5, which is consistent with the leading term in the theoretical estimation errors $O\left[T^{1.5} + T\sqrt{\ln(T)} + T\right]$ derived from Eqs. (29)-(31). These results confirm that the increase in the estimation error of the neural oscillator with respect to the time length T is moderate.

The ODE of the extreme value process $E_{X_5}(t)$ can be expressed as

$$E'_{X_5}(t) = \begin{cases} |X'_5(t)|, & |X_5(t)| \geq E_{X_5}(t) \\ 0, & \text{otherwise} \end{cases}. \quad (38)$$

By incorporating Eq. (38) into Eq. (33), it can be shown that the mapping from $U_e(t)$ to $E_{X_5}(t)$ is continuous but not smooth due to the piecewise nature of the derivative term in Eq. (38). This nonsmoothness renders the learning of this mapping more difficult than that of the smooth one from $U_e(t)$ to $X_5(t)$. Figures 3 and 4 respectively compare the probability density functions (PDFs) and cumulative distribution functions (CDFs) of $E_{X_5}(t)$ at $T = 30$ estimated from the 5×10^4 samples $E_{X_5,t}(t_i)$ and $\tilde{E}_{X_5,t}(t_i)$. The results indicate that the neural oscillator trained with 1600 samples can accurately predict the probability distribution of $E_{X_5}(30)$, demonstrating its ability to effectively approximate the nonsmooth mapping from $U_e(t)$ to $E_{X_5}(t)$.

5. Conclusions

In this study, two upper PAC generalization bounds of the neural oscillator consisting of a second-order ODE followed by an MLP are derived for approximating the causal and uniformly continuous operators between continuous temporal function spaces and for approximating the uniformly asymptotically incrementally stable second-order dynamical systems. The theoretical results demonstrate that the estimation errors in the generalization bounds grow polynomially with increasing MLP sizes and time length, thereby avoiding the curse of parametric complexity. Moreover, the derived generalization bounds reveal that the generalization capability of the neural oscillator can be enhanced by constraining the Lipschitz constants of the employed MLPs through appropriate regularization in the loss function. A numerical study based on a Bouc-Wen nonlinear system subjected to stochastic seismic excitation validates the power laws of the estimation errors with respect to the sample size and time length, and confirms the effectiveness of constraining the MLPs' matrix and vector norms in improving the generalization performance of the neural oscillator under limited training data.

CRedit authorship contribution statement

Zifeng Huang: Conceptualization, Methodology, Software, Writing-reviewing & editing, Project administration. **Konstantin M. Zuev:** Methodology, Writing-reviewing & editing. **Yong Xia:** Writing-reviewing & editing, Supervision. **Michael Beer:** Supervision, Project administration.

Declaration of competing interest

The authors declare that they have no known competing financial interests or personal relationships that could have appeared to influence the work reported in this paper.

Data and Code Availability

All code used in this study is available at: <https://github.com/ZifengH22/Upper-Generalization-Bounds-for-Neural-Oscillators>. All data presented in this study were generated using this code.

Acknowledgments

This work is supported by the German Research Foundation (Project No. 554325683 and HU 3418/2-1). The opinions and conclusions presented in this paper are entirely those of the authors.

Appendix A. Proofs for Lemmas and Theorems in Section 3

Appendix A.1. Proof of Lemma 3

Proof: The empirical Rademacher complexity $\mathfrak{R}_{\mathcal{G}_\theta}$ in Eq. (15) can be calculated as

$$\mathfrak{R}_{\mathcal{G}_\theta} = \mathbb{E}_\sigma \sup_{\Pi \circ \Phi_\Gamma \in \mathcal{F}_{\Pi \circ \Phi_\Gamma}} \frac{1}{N} \sum_{i=1}^N \sigma_i \sum_{j=1}^{w_{\Pi, \text{out}}} \int_0^T \left\{ v_{ij}(t) - \Pi \circ \Phi_\Gamma[\mathbf{u}_i(\tau)]_j(t) \right\}^2 dt, \quad (\text{A.1})$$

where $v_{ij}(t) = \Phi[\mathbf{u}_i(\tau)]_j(t)$ and $\Pi \circ \Phi_\Gamma[\mathbf{u}_i(\tau)]_j(t)$ are the j^{th} elements of the q -dimensional vector functions $\Phi[\mathbf{u}_i(\tau)](t)$ and $\Pi \circ \Phi_\Gamma[\mathbf{u}_i(\tau)](t)$, respectively, and $q = w_{\Pi, \text{out}}$. Since $\Pi \circ \Phi_\Gamma[\mathbf{u}_i(\tau)]_j(t)$ and $v_{ij}(t)$ are bounded and continuous functions over $[0, T]$, they can be respectively expressed as

$$\Pi \circ \Phi_\Gamma[\mathbf{u}_i(\tau)]_j(t) = \sum_{k=1}^{+\infty} \alpha_{jk} \left\{ \Pi \circ \Phi_\Gamma[\mathbf{u}_i(\tau)]_j \right\} e_k(t) \quad (\text{A.2})$$

and

$$v_{ij}(t) = \sum_{k=1}^{+\infty} \beta_{jk}(v_{ij}) e_k(t), \quad (\text{A.3})$$

where $e_k(t)$, $k = 1, 2, \dots$, denote a countable set of standard orthogonal basis functions over $[0, T]$, $\alpha_{jk} \left\{ \Pi \circ \Phi_\Gamma[\mathbf{u}_i(\tau)]_j \right\}$ and $\beta_{jk}(v_{ij})$ are the coefficients of $\Pi \circ \Phi_\Gamma[\mathbf{u}_i(\tau)]_j(t)$ and $v_{ij}(t)$, respectively.

Substituting Eqs. (A.2) and (A.3) in Eq. (A.1) and utilizing the Parseval's identity, $\mathfrak{R}_{\mathcal{G}_\theta}$ can be expressed as

$$\begin{aligned} \mathfrak{R}_{\mathcal{G}_\theta} &= \mathbb{E}_\sigma \sup_{\Pi \circ \Phi_\Gamma \in \mathcal{F}_{\Pi \circ \Phi_\Gamma}} \frac{1}{N} \sum_{i=1}^N \sigma_i \sum_{j=1}^{w_{\Pi, \text{out}}} \int_0^T \left[\sum_{k=1}^{+\infty} \left(\beta_{jk}(v_{ij}) - \alpha_{jk} \left\{ \Pi \circ \Phi_\Gamma[\mathbf{u}_i(\tau)]_j \right\} \right) e_k(t) \right]^2 dt \\ &= \mathbb{E}_\sigma \sup_{\Pi \circ \Phi_\Gamma \in \mathcal{F}_{\Pi \circ \Phi_\Gamma}} \frac{1}{N} \sum_{i=1}^N \sigma_i z \{ \Pi \circ \Phi_\Gamma[\mathbf{u}_i(\tau)] \}, \end{aligned} \quad (\text{A.4})$$

where

$$z \{ \Pi \circ \Phi_\Gamma[\mathbf{u}_i(\tau)] \} = \sum_{j=1}^{w_{\Pi, \text{out}}} \sum_{k=1}^{+\infty} \left(\beta_{jk}(v_{ij}) - \alpha_{jk} \left\{ \Pi \circ \Phi_\Gamma[\mathbf{u}_i(\tau)]_j \right\} \right)^2. \quad (\text{A.5})$$

Consider two neural oscillators $\Pi_1 \circ \Phi_{\Gamma_1}$ and $\Pi_2 \circ \Phi_{\Gamma_2} \in \mathcal{F}_{\Pi \circ \Phi_{\Gamma}}$, the difference between $z\{\Pi_1 \circ \Phi_{\Gamma_1}[\mathbf{u}_i(\tau)]_j(t)\}$ and $z\{\Pi_2 \circ \Phi_{\Gamma_2}[\mathbf{u}_i(\tau)]_j(t)\}$ can be bounded by

$$\begin{aligned}
& \left| z\{\Pi_1 \circ \Phi_{\Gamma_1}[\mathbf{u}_i(\tau)]_j\} - z\{\Pi_2 \circ \Phi_{\Gamma_2}[\mathbf{u}_i(\tau)]_j\} \right| \\
&= \left| \sum_{j=1}^{w_{\Pi, \text{out}}} \sum_{k=1}^{+\infty} (\beta_{jk}(v_{ij}) - \alpha_{jk} \{\Pi_1 \circ \Phi_{\Gamma_1}[\mathbf{u}_i(\tau)]_j\})^2 - \sum_{j=1}^{w_{\Pi, \text{out}}} \sum_{k=1}^{+\infty} (\beta_{jk}(v_{ij}) - \alpha_{jk} \{\Pi_2 \circ \Phi_{\Gamma_2}[\mathbf{u}_i(\tau)]_j\})^2 \right| \\
&= \left| \sum_{j=1}^{w_{\Pi, \text{out}}} \sum_{k=1}^{+\infty} (\alpha_{jk}^2 \{\Pi_1 \circ \Phi_{\Gamma_1}[\mathbf{u}_i(\tau)]_j\} - \alpha_{jk}^2 \{\Pi_2 \circ \Phi_{\Gamma_2}[\mathbf{u}_i(\tau)]_j\}) \right. \\
&\quad \left. - 2 \sum_{j=1}^{w_{\Pi, \text{out}}} \sum_{k=1}^{+\infty} \beta_{jk}(v_{ij}) (\alpha_{jk} \{\Pi_1 \circ \Phi_{\Gamma_1}[\mathbf{u}_i(\tau)]_j\} - \alpha_{jk} \{\Pi_2 \circ \Phi_{\Gamma_2}[\mathbf{u}_i(\tau)]_j\}) \right| \\
&= \left| \sum_{j=1}^{w_{\Pi, \text{out}}} \sum_{k=1}^{+\infty} (\alpha_{jk} \{\Pi_1 \circ \Phi_{\Gamma_1}[\mathbf{u}_i(\tau)]_j\} - \alpha_{jk} \{\Pi_2 \circ \Phi_{\Gamma_2}[\mathbf{u}_i(\tau)]_j\}) \right. \\
&\quad \left. \times (\alpha_{jk} \{\Pi_1 \circ \Phi_{\Gamma_1}[\mathbf{u}_i(\tau)]_j\} + \alpha_{jk} \{\Pi_2 \circ \Phi_{\Gamma_2}[\mathbf{u}_i(\tau)]_j\} - 2\beta_{jk}(v_{ij})) \right| \\
&\stackrel{(a)}{\leq} \sqrt{\sum_{j=1}^{w_{\Pi, \text{out}}} \sum_{k=1}^{+\infty} (\alpha_{jk} \{\Pi_1 \circ \Phi_{\Gamma_1}[\mathbf{u}_i(\tau)]_j\} - \alpha_{jk} \{\Pi_2 \circ \Phi_{\Gamma_2}[\mathbf{u}_i(\tau)]_j\})^2} \\
&\quad \times \sqrt{\sum_{j=1}^{w_{\Pi, \text{out}}} \sum_{k=1}^{+\infty} (\alpha_{jk} \{\Pi_1 \circ \Phi_{\Gamma_1}[\mathbf{u}_i(\tau)]_j\} + \alpha_{jk} \{\Pi_2 \circ \Phi_{\Gamma_2}[\mathbf{u}_i(\tau)]_j\} - 2\beta_{jk}(v_{ij}))^2} \\
&= \sqrt{\sum_{j=1}^{w_{\Pi, \text{out}}} \sum_{k=1}^{+\infty} (\alpha_{jk} \{\Pi_1 \circ \Phi_{\Gamma_1}[\mathbf{u}_i(\tau)]_j\} - \alpha_{jk} \{\Pi_2 \circ \Phi_{\Gamma_2}[\mathbf{u}_i(\tau)]_j\})^2} \\
&\quad \times \sqrt{\sum_{j=1}^{w_{\Pi, \text{out}}} \int_0^T \{\Pi_1 \circ \Phi_{\Gamma_1}[\mathbf{u}_i(\tau)]_j(t) + \Pi_2 \circ \Phi_{\Gamma_2}[\mathbf{u}_i(\tau)]_j(t) - 2v_{ij}(t)\}^2 dt} \\
&\stackrel{(b)}{\leq} 2\sqrt{T w_{\Pi, \text{out}} B_{\text{loss}}} \sqrt{\sum_{j=1}^{w_{\Pi, \text{out}}} \sum_{k=1}^{+\infty} (\alpha_{jk} \{\Pi_1 \circ \Phi_{\Gamma_1}[\mathbf{u}_i(\tau)]_j\} - \alpha_{jk} \{\Pi_2 \circ \Phi_{\Gamma_2}[\mathbf{u}_i(\tau)]_j\})^2}, \tag{A.6}
\end{aligned}$$

where Step (a) follows from the Cauchy-Schwarz inequality and Step (b) relies on the Assumption 11 that $|\Pi_1 \circ \Phi_{\Gamma_1}[\mathbf{u}_i(\tau)]_j + \Pi_2 \circ \Phi_{\Gamma_2}[\mathbf{u}_i(\tau)]_j - 2v_{ij}(t)|$ is bounded by $2B_{\text{loss}}$. Eq. (A.6) indicates that $2\sqrt{T w_{\Pi, \text{out}} B_{\text{loss}}}$ is a Lipschitz constant of $z\{\Pi \circ \Phi_{\Gamma}[\mathbf{u}_i(\tau)]_j\}$ with respect to $\alpha_{jk} \{\Pi \circ \Phi_{\Gamma}[\mathbf{u}_i(\tau)]_j\}$. Then, from Corollary 4 of Maurer (2016) and Eq. (A.4), $\mathfrak{R}_{\mathcal{G}_{\theta}}$ can be bounded by

$$\mathfrak{R}_{\mathcal{G}_{\theta}} \leq \mathbb{E}_{\tilde{\sigma}} \sup_{\Pi \circ \Phi_{\Gamma} \in \mathcal{F}_{\Pi \circ \Phi_{\Gamma}}} \frac{2\sqrt{2T w_{\Pi, \text{out}} B_{\text{loss}}}}{N} \sum_{i=1}^N \sum_{j=1}^{w_{\Pi, \text{out}}} \sum_{k=1}^{+\infty} \tilde{\sigma}_{ijk} \alpha_{jk} \{\Pi \circ \Phi_{\Gamma}[\mathbf{u}_i(\tau)]_j\}. \tag{A.7}$$

This completes the proof. ■

Appendix A.2. Proof of Lemma 4

Proof: Consider a random variable sequence X_K , $K = 1, 2, \dots$

$$X_K = \sum_{i=1}^N \sum_{j=1}^{w_{\Pi, \text{out}}} \sum_{k=1}^K \tilde{\sigma}_{ijk} \alpha_{ijk}, \tag{A.8}$$

where $\alpha_{ijk} = \alpha_{jk} \{\Pi \circ \Phi_{\Gamma}[\mathbf{u}_i(\tau)]_j\}$ for $\forall \Pi \circ \Phi_{\Gamma} \in \mathcal{F}_{\Pi \circ \Phi_{\Gamma}}$, this sequence satisfies

$$\begin{aligned}
\lim_{K_1, K_2 \rightarrow +\infty} \mathbb{E}_{\tilde{\sigma}} (X_{K_2} - X_{K_1})^2 &= \lim_{K_1, K_2 \rightarrow +\infty} \mathbb{E}_{\tilde{\sigma}} \left(\sum_{i=1}^N \sum_{j=1}^{w_{\Pi, \text{out}}} \sum_{k=1}^{K_2} \tilde{\sigma}_{ijk} \alpha_{ijk} - \sum_{i=1}^N \sum_{j=1}^{w_{\Pi, \text{out}}} \sum_{k=1}^{K_1} \tilde{\sigma}_{ijk} \alpha_{ijk} \right)^2 \\
&\stackrel{(a)}{=} \lim_{K_{\min}, K_{\max} \rightarrow +\infty} \sum_{i=1}^N \sum_{j=1}^{w_{\Pi, \text{out}}} \sum_{k=K_{\min}+1}^{K_{\max}} \alpha_{ijk}^2 \stackrel{(b)}{=} 0, \tag{A.9}
\end{aligned}$$

where in Step (a) $K_{\min} = \min(K_1, K_2)$ and $K_{\max} = \max(K_1, K_2)$, and Step (b) is valid since the sequence α_{ijk} is square-summable. Eq. (A.9) indicates that the sequence X_K converges in mean-square. The expectation of $\kappa(\Pi \circ \Phi_{\Gamma}, \tilde{\sigma})$ is

$$\mathbb{E}_{\tilde{\sigma}} \kappa(\Pi \circ \Phi_{\Gamma}, \tilde{\sigma}) = \mathbb{E}_{\tilde{\sigma}} \sum_{i=1}^N \sum_{j=1}^{w_{\Pi, \text{out}}} \sum_{k=1}^{+\infty} \tilde{\sigma}_{ijk} \alpha_{ijk} \stackrel{(a)}{=} \sum_{i=1}^N \sum_{j=1}^{w_{\Pi, \text{out}}} \sum_{k=1}^{+\infty} \mathbb{E}_{\tilde{\sigma}} \tilde{\sigma}_{ijk} \alpha_{ijk} = 0, \quad (\text{A.10})$$

where the mean-square convergence property of X_K allows the expectation and limit to be interchanged in Step (a) (Huang and Xia, 2022).

For arbitrary $\Pi_1 \circ \Phi_{\Gamma_1}, \Pi_2 \circ \Phi_{\Gamma_2} \in \mathcal{F}_{\Pi \circ \Phi_{\Gamma}}, \Pi_1 \circ \Phi_{\Gamma_1} [\mathbf{u}_i(\tau)]_j(t) - \Pi_2 \circ \Phi_{\Gamma_2} [\mathbf{u}_i(\tau)]_j(t)$ are bounded and continuous functions over $[0, T]$ for all $i = 1, 2, \dots, N$ and $j = 1, 2, \dots, w_{\Pi, \text{out}}$. Thus, $\Delta\alpha_{ijk} = \alpha_{ijk,1} - \alpha_{ijk,2}$ is also a square-summable sequence, where $\alpha_{ijk,1} = \alpha_{jk} \{ \Pi_1 \circ \Phi_{\Gamma_1} [\mathbf{u}_i(\tau)]_j \}$ and $\alpha_{ijk,2} = \alpha_{jk} \{ \Pi_2 \circ \Phi_{\Gamma_2} [\mathbf{u}_i(\tau)]_j \}$. $X_{K,\Delta} = \sum_{i=1}^N \sum_{j=1}^{w_{\Pi, \text{out}}} \sum_{k=1}^K \tilde{\sigma}_{ijk} \Delta\alpha_{ijk}$ is a sequence converging in mean-square and satisfies

$$\mathbb{E}_{\tilde{\sigma}} \left(\lim_{K \rightarrow +\infty} X_{K,\Delta} \right)^2 = \lim_{K \rightarrow +\infty} \mathbb{E}_{\tilde{\sigma}} X_{K,\Delta}^2. \quad (\text{A.11})$$

The pseudo-metric $d_k(\Pi_1 \circ \Phi_{\Gamma_1}, \Pi_2 \circ \Phi_{\Gamma_2})$ for arbitrary $\Pi_1 \circ \Phi_{\Gamma_1}, \Pi_2 \circ \Phi_{\Gamma_2} \in \mathcal{F}_{\Pi \circ \Phi_{\Gamma}}$ is calculated as

$$\begin{aligned} d_k(\Pi_1 \circ \Phi_{\Gamma_1}, \Pi_2 \circ \Phi_{\Gamma_2}) &= \sqrt{\mathbb{E}_{\tilde{\sigma}} [\kappa(\Pi_1 \circ \Phi_{\Gamma_1}, \tilde{\sigma}) - \kappa(\Pi_2 \circ \Phi_{\Gamma_2}, \tilde{\sigma})]^2} = \sqrt{\mathbb{E}_{\tilde{\sigma}} \left[\sum_{i=1}^N \sum_{j=1}^{w_{\Pi, \text{out}}} \sum_{k=1}^{+\infty} \tilde{\sigma}_{ijk} \Delta\alpha_{ijk} \right]^2} \\ &\stackrel{(a)}{=} \sqrt{\sum_{i=1}^N \sum_{j=1}^{w_{\Pi, \text{out}}} \sum_{k=1}^{+\infty} \mathbb{E}_{\tilde{\sigma}} \tilde{\sigma}_{ijk}^2 \Delta\alpha_{ijk}^2} = \sqrt{\sum_{i=1}^N \sum_{j=1}^{w_{\Pi, \text{out}}} \sum_{k=1}^{+\infty} \Delta\alpha_{ijk}^2} \\ &= \sqrt{\sum_{i=1}^N \sum_{j=1}^{w_{\Pi, \text{out}}} \int_0^T \{ \Pi_1 \circ \Phi_{\Gamma_1} [\mathbf{u}_i(\tau)]_j(t) - \Pi_2 \circ \Phi_{\Gamma_2} [\mathbf{u}_i(\tau)]_j(t) \}^2 dt} \\ &= \sqrt{\sum_{i=1}^N \| \Pi_1 \circ \Phi_{\Gamma_1} [\mathbf{u}_i(\tau)](t) - \Pi_2 \circ \Phi_{\Gamma_2} [\mathbf{u}_i(\tau)](t) \|_{L^2}^2}, \end{aligned} \quad (\text{A.12})$$

where Step (a) holds from Eq. (A.11). Given $\forall w \in \mathbb{R}$, it can be obtained

$$\begin{aligned} &\mathbb{E}_{\tilde{\sigma}} \exp \{ w [\kappa(\Pi_1 \circ \Phi_{\Gamma_1}, \tilde{\sigma}) - \kappa(\Pi_2 \circ \Phi_{\Gamma_2}, \tilde{\sigma})] \} \\ &= \mathbb{E}_{\tilde{\sigma}} \exp \left(w \sum_{i=1}^N \sum_{j=1}^{w_{\Pi, \text{out}}} \sum_{k=1}^{+\infty} \tilde{\sigma}_{ijk} \Delta\alpha_{ijk} \right) \stackrel{(a)}{=} \prod_{i=1}^N \prod_{j=1}^{w_{\Pi, \text{out}}} \prod_{k=1}^{+\infty} E_{\tilde{\sigma}_{ijk}} \exp \left(\tilde{\sigma}_{ijk} w \Delta\alpha_{ijk} \right) \\ &\stackrel{(b)}{\leq} \prod_{i=1}^N \prod_{j=1}^{w_{\Pi, \text{out}}} \prod_{k=1}^{+\infty} \exp \left(0.5 w^2 \Delta\alpha_{ijk}^2 \right) = \exp \left(0.5 w^2 \sum_{i=1}^N \sum_{j=1}^{w_{\Pi, \text{out}}} \sum_{k=1}^{+\infty} \Delta\alpha_{ijk}^2 \right) \\ &\stackrel{(c)}{=} \exp \left[0.5 w^2 d_k^2(\Pi_1 \circ \Phi_{\Gamma_1}, \Pi_2 \circ \Phi_{\Gamma_2}) \right], \end{aligned} \quad (\text{A.13})$$

where Step (b) is valid because of Lemma A.6 in Shalev-Shwartz and Ben-David (2014) that for $\forall a \in \mathbb{R}$, it is satisfied $\mathbb{E}_{\tilde{\sigma}_{ijk}} \exp(\tilde{\sigma}_{ijk} a) = 0.5 [\exp(a) + \exp(-a)] \leq \exp(0.5a^2)$, Step (c) is from Eq. (A.12), and Step (a) is demonstrated as follows.

A random variable sequence $Y_K, K = 1, 2, \dots$, is defined as

$$Y_K = \exp \left(w \sum_{i=1}^N \sum_{j=1}^{w_{\Pi, \text{out}}} \sum_{k=1}^K \tilde{\sigma}_{ijk} \Delta\alpha_{ijk} \right). \quad (\text{A.14})$$

This sequence satisfies

$$\begin{aligned}
& \lim_{K_1, K_2 \rightarrow +\infty} \mathbb{E}_{\tilde{\sigma}} Y_{K_1} Y_{K_2} \\
&= \lim_{K_1, K_2 \rightarrow +\infty} \mathbb{E}_{\tilde{\sigma}} \exp\left(w \sum_{i=1}^N \sum_{j=1}^{w_{\Pi, \text{out}}} \sum_{k=1}^{K_1} \tilde{\sigma}_{ijk} \Delta \alpha_{ijk}\right) \exp\left(w \sum_{i=1}^N \sum_{j=1}^{w_{\Pi, \text{out}}} \sum_{k=1}^{K_2} \tilde{\sigma}_{ijk} \Delta \alpha_{ijk}\right) \\
&\stackrel{(a)}{=} \lim_{K_{\min}, K_{\max} \rightarrow +\infty} \mathbb{E}_{\tilde{\sigma}} \exp\left[w \left(2 \sum_{i=1}^N \sum_{j=1}^{w_{\Pi, \text{out}}} \sum_{k=1}^{K_{\min}} \tilde{\sigma}_{ijk} \Delta \alpha_{ijk} + \sum_{i=1}^N \sum_{j=1}^{w_{\Pi, \text{out}}} \sum_{k=K_{\min}+1}^{K_{\max}} \tilde{\sigma}_{ijk} \Delta \alpha_{ijk}\right)\right] \\
&= \lim_{K_{\min}, K_{\max} \rightarrow +\infty} \mathbb{E}_{\tilde{\sigma}} \exp\left(2w \sum_{i=1}^N \sum_{j=1}^{w_{\Pi, \text{out}}} \sum_{k=1}^{K_{\min}} \tilde{\sigma}_{ijk} \Delta \alpha_{ijk}\right) \mathbb{E}_{\tilde{\sigma}} \exp\left(w \sum_{i=1}^N \sum_{j=1}^{w_{\Pi, \text{out}}} \sum_{k=K_{\min}+1}^{K_{\max}} \tilde{\sigma}_{ijk} \Delta \alpha_{ijk}\right) \\
&= \lim_{K_{\min}, K_{\max} \rightarrow +\infty} A_{K_{\min}} B_{K_{\min}}^{K_{\max}},
\end{aligned} \tag{A.15}$$

where

$$A_{K_{\min}} = \prod_{i=1}^N \prod_{j=1}^{w_{\Pi, \text{out}}} \prod_{k=1}^{K_{\min}} 0.5 \left[\exp(2w \Delta \alpha_{ijk}) + \exp(-2w \Delta \alpha_{ijk}) \right] \leq \exp\left(2w^2 \sum_{i=1}^N \sum_{j=1}^{w_{\Pi, \text{out}}} \sum_{k=1}^{K_{\min}} \Delta \alpha_{ijk}^2\right), \tag{A.16}$$

$$1 \leq B_{K_{\min}}^{K_{\max}} = \prod_{i=1}^N \prod_{j=1}^{w_{\Pi, \text{out}}} \prod_{k=K_{\min}+1}^{K_{\max}} 0.5 \left[\exp(w \Delta \alpha_{ijk}) + \exp(-w \Delta \alpha_{ijk}) \right] \leq \exp\left(0.5w^2 \sum_{i=1}^N \sum_{j=1}^{w_{\Pi, \text{out}}} \sum_{k=K_{\min}+1}^{K_{\max}} \Delta \alpha_{ijk}^2\right), \tag{A.17}$$

and in Step (a) of Eq. (A.15) $K_{\min} = \min(K_1, K_2)$ and $K_{\max} = \max(K_1, K_2)$. Since the sequence $\Delta \alpha_{ijk}$ is square-summable and $0.5 [\exp(a) + \exp(-a)] \geq 1$ for all $a \in \mathbb{R}$, $A_{K_{\min}}$ is a monotonically increasing and bounded sequence with respect to K_{\min} , and its limit exists. $B_{K_{\min}}^{K_{\max}}$ is also a bounded sequence with respect to K_{\min} and K_{\max} , and its limit is 1 because of $1 = \lim_{K_{\min}, K_{\max} \rightarrow +\infty} \exp\left(0.5w^2 \sum_{i=1}^N \sum_{j=1}^{w_{\Pi, \text{out}}} \sum_{k=K_{\min}+1}^{K_{\max}} \Delta \alpha_{ijk}^2\right) \geq \lim_{K_{\min}, K_{\max} \rightarrow +\infty} B_{K_{\min}}^{K_{\max}} \geq 1$. Since the values of $A_{K_{\min}}$ and $B_{K_{\min}}^{K_{\max}}$ are bounded, the limit in Eq. (A.15) exists and equals that of $A_{K_{\min}}$, and it is independent of the manner in which K_{\min} and K_{\max} approach infinity. It is also independent of the manner in which K_1 and K_2 approach infinity. Thus, it can be obtained $\lim_{K_1, K_2 \rightarrow +\infty} \mathbb{E}_{\tilde{\sigma}} (Y_{K_2} - Y_{K_1})^2 = \lim_{K_1, K_2 \rightarrow +\infty} \mathbb{E}_{\tilde{\sigma}} (Y_{K_1}^2 + Y_{K_2}^2 - Y_{K_1} Y_{K_2} - Y_{K_2} Y_{K_1}) = 0$. This result indicates that the random variable sequence Y_K converges in mean-square, thereby allowing the expectation and limit to be interchanged in Step (a) of Eq. (A.13) (Huang and Xia, 2022).

Eqs. (A.10) and (A.13) prove that $\kappa(\Pi \circ \Phi_{\Gamma}, \tilde{\sigma})$ is a zero-mean sub-Gaussian process with respect to $\Pi \circ \Phi_{\Gamma}$ over $\mathcal{F}_{\Pi \circ \Phi_{\Gamma}}$. The diameter of $\kappa(\Pi \circ \Phi_{\Gamma}, \tilde{\sigma})$ over $\mathcal{F}_{\Pi \circ \Phi_{\Gamma}}$ is bounded by

$$\Delta_{\kappa}(\mathcal{F}_{\Pi \circ \Phi_{\Gamma}}) = \sup_{\Pi_1 \circ \Phi_{\Gamma_1}, \Pi_2 \circ \Phi_{\Gamma_2} \in \mathcal{F}_{\Pi \circ \Phi_{\Gamma}}} d_{\kappa}(\Pi_1 \circ \Phi_{\Gamma_1}, \Pi_2 \circ \Phi_{\Gamma_2}) \stackrel{(a)}{\leq} 2 \sqrt{NT w_{\Pi, \text{out}}} B_{\Pi}, \tag{A.18}$$

where Step (a) holds from Eq. (A.12). ■

Appendix A.3. Proof of Lemma 5

Proof: For $\forall \Gamma(\cdot) \in \mathcal{F}_{\Gamma}$, the difference between $\Gamma(\mathbf{x}_1)$ and $\Gamma(\mathbf{x}_2)$ is bounded by

$$\begin{aligned}
|\Gamma(\mathbf{x}_1) - \Gamma(\mathbf{x}_2)| &= |\mathbf{W}_2 [\sigma_{\text{ReLU}}(\mathbf{W}_1 \mathbf{x}_1 + \mathbf{b}_1) - \sigma_{\text{ReLU}}(\mathbf{W}_1 \mathbf{x}_2 + \mathbf{b}_1)]| \\
&\leq \|\mathbf{W}_2\|_{\infty, 1} |\sigma_{\text{ReLU}}(\mathbf{W}_1 \mathbf{x}_1 + \mathbf{b}_1) - \sigma_{\text{ReLU}}(\mathbf{W}_1 \mathbf{x}_2 + \mathbf{b}_1)| \\
&\leq w_{\Gamma, \text{out}} \|\mathbf{W}_2\|_{\infty, \infty} \|\mathbf{W}_1(\mathbf{x}_1 - \mathbf{x}_2)\| \\
&\leq w_{\Gamma, \text{out}} \|\mathbf{W}_2\|_{\infty, \infty} \|\mathbf{W}_1\|_{\infty, \infty} w_{\Gamma} \|\mathbf{x}_1 - \mathbf{x}_2\| \leq w_{\Gamma, \text{out}} w_{\Gamma} B_{\mathbf{W}}^2 \|\mathbf{x}_1 - \mathbf{x}_2\|.
\end{aligned} \tag{A.19}$$

Thus, $L_{\mathcal{F}_{\Gamma}} = w_{\Gamma, \text{out}} w_{\Gamma} B_{\mathbf{W}}^2$ is an L^1 -norm Lipschitz constant of all $\Gamma(\cdot) \in \mathcal{F}_{\Gamma}$. For $\forall \Pi(\cdot) \in \mathcal{F}_{\Pi}$, the difference between $\Pi(\mathbf{x}_1)$ and $\Pi(\mathbf{x}_2)$ is bounded by

$$\begin{aligned}
|\Pi(\mathbf{x}_1) - \Pi(\mathbf{x}_2)| &\leq \|\tilde{\mathbf{W}}_{\Pi}^{\text{T}}\|_{\infty, 1} \left| \sigma_{\text{ReLU}} \left[\dots \sigma_{\text{ReLU}}(\tilde{\mathbf{W}}_1 \mathbf{x}_1 + \tilde{\mathbf{b}}_1) \right] - \sigma_{\text{ReLU}} \left[\dots \sigma_{\text{ReLU}}(\tilde{\mathbf{W}}_1 \mathbf{x}_2 + \tilde{\mathbf{b}}_1) \right] \right| \\
&\leq w_{\Pi, \text{out}} B_{\tilde{\mathbf{W}}} \left| \sigma_{\text{ReLU}} \left[\dots \sigma_{\text{ReLU}}(\tilde{\mathbf{W}}_1 \mathbf{x}_1 + \tilde{\mathbf{b}}_1) \right] - \sigma_{\text{ReLU}} \left[\dots \sigma_{\text{ReLU}}(\tilde{\mathbf{W}}_1 \mathbf{x}_2 + \tilde{\mathbf{b}}_1) \right] \right| \\
&\leq w_{\Pi, \text{out}} w_{\Pi}^{h_{\Pi}-1} B_{\tilde{\mathbf{W}}}^{h_{\Pi}} \|\mathbf{x}_1 - \mathbf{x}_2\|.
\end{aligned} \tag{A.20}$$

Thus, $L_{\mathcal{F}_{\Pi}} = w_{\Pi, \text{out}} w_{\Pi}^{h_{\Pi}-1} B_{\tilde{\mathbf{W}}}^{h_{\Pi}}$ is an L^1 -norm Lipschitz constant of all $\Pi(\cdot) \in \mathcal{F}_{\Pi}$. ■

Appendix A.4. Proof of Lemma 6

Proof: Since the weight matrices and vectors of all $\Gamma(\cdot) \in \mathcal{F}_T$ in Assumption 9 are bounded and $\sigma_{\text{ReLU}}(\cdot)$ is Lipschitz continuous, the first ODE in Eq. (1) with the initial conditions $\mathbf{x}(0) = \mathbf{x}'(0) = \mathbf{0}$ has unique solutions $\mathbf{x}(t) = \Phi_T[\mathbf{u}(\tau)](t)$ for all $\mathbf{u}(t) \in K$. $\mathbf{x}(t)$ and its derivative $\mathbf{x}'(t)$ satisfy

$$\begin{aligned} |\mathbf{x}(t)| + |\mathbf{x}'(t)| &= \left| \int_0^t \mathbf{x}'(\tau) d\tau \right| + \left| \int_0^t \Gamma[\mathbf{x}(\tau), \mathbf{x}'(\tau), \mathbf{u}(\tau)] d\tau \right| \leq \int_0^t |\mathbf{x}'(\tau)| d\tau + \int_0^t |\Gamma[\mathbf{x}(\tau), \mathbf{x}'(\tau), \mathbf{u}(\tau)]| d\tau \\ &\stackrel{(a)}{\leq} \int_0^t |\mathbf{x}'(\tau)| d\tau + L_{\mathcal{F}_T} \int_0^t [|\mathbf{x}(\tau)| + |\mathbf{x}'(\tau)| + |\mathbf{u}(\tau)|] d\tau + \int_0^t |\Gamma(\mathbf{0})| d\tau \\ &\leq (L_{\mathcal{F}_T} + 1) \int_0^t [|\mathbf{x}(\tau)| + |\mathbf{x}'(\tau)|] d\tau + pTB_K L_{\mathcal{F}_T} + T [|\mathbf{W}_2 \sigma_{\text{ReLU}}(\mathbf{b}_1)| + |\mathbf{b}_2|] \\ &\leq (L_{\mathcal{F}_T} + 1) \int_0^t [|\mathbf{x}(\tau)| + |\mathbf{x}'(\tau)|] d\tau + T [pB_K L_{\mathcal{F}_T} + w_{\Gamma, \text{out}} B_{\mathbf{b}} (w_{\Gamma} B_{\mathbf{W}} + 1)] \\ &\stackrel{(b)}{\leq} T [pB_K L_{\mathcal{F}_T} + w_{\Gamma, \text{out}} B_{\mathbf{b}} (w_{\Gamma} B_{\mathbf{W}} + 1)] e^{T(L_{\mathcal{F}_T} + 1)}, \end{aligned} \quad (\text{A.21})$$

where in Step (a) $L_{\mathcal{F}_T}$ is an arbitrary L^1 -norm Lipschitz constant for all $\Gamma(\cdot) \in \mathcal{F}_T$ and Step (b) is from the Grönwall's inequality (Ames and Pachpatte, 1997). \blacksquare

Appendix A.5. Proof of Lemma 7

Proof: As explained in the proof of Lemma 6, $\mathbf{x}_1(t) = \Phi_{\Gamma_1}[\mathbf{u}(\tau)](t)$ and $\mathbf{x}_2(t) = \Phi_{\Gamma_2}[\mathbf{u}(\tau)](t)$ are unique solutions of the first ODE in Eq. (1) for all $\mathbf{u}(t) \in K$. From Appendix D and Lemma 6 in Huang et al. (2025), $|\mathbf{x}_2(t) - \mathbf{x}_1(t)|$ can be bounded by

$$|\mathbf{x}_2(t) - \mathbf{x}_1(t)| \leq e^{T(L_{\mathcal{F}_T} + 1)} T \max_{\tau \in [0, T]} \left| \Gamma_2[\mathbf{x}_2(\tau), \mathbf{x}'_2(\tau), \mathbf{u}(\tau)] - \Gamma_1[\mathbf{x}_2(\tau), \mathbf{x}'_2(\tau), \mathbf{u}(\tau)] \right|, \quad (\text{A.22})$$

where $L_{\mathcal{F}_T}$ is an arbitrary L^1 -norm Lipschitz constant that simultaneously bounds all $\Gamma(\cdot) \in \mathcal{F}_T$. $|\Gamma_2[\mathbf{x}_2(\tau), \mathbf{x}'_2(\tau), \mathbf{u}(\tau)] - \Gamma_1[\mathbf{x}_2(\tau), \mathbf{x}'_2(\tau), \mathbf{u}(\tau)]|$ in Eq. (A.22) can be bounded by

$$\begin{aligned} &\left| \Gamma_2[\mathbf{x}_2(\tau), \mathbf{x}'_2(\tau), \mathbf{u}(\tau)] - \Gamma_1[\mathbf{x}_2(\tau), \mathbf{x}'_2(\tau), \mathbf{u}(\tau)] \right| \\ &\leq \left| \mathbf{W}_{2,2} \sigma_{\text{ReLU}} \left\{ \mathbf{W}_{2,1} [\mathbf{x}_2^\top(\tau), \mathbf{x}'_2^\top(\tau), \mathbf{u}^\top(\tau)]^\top + \mathbf{b}_{2,1} \right\} + \mathbf{b}_{2,2} \right. \\ &\quad \left. - \mathbf{W}_{1,2} \sigma_{\text{ReLU}} \left\{ \mathbf{W}_{1,1} [\mathbf{x}_2^\top(\tau), \mathbf{x}'_2^\top(\tau), \mathbf{u}^\top(\tau)]^\top + \mathbf{b}_{1,1} \right\} - \mathbf{b}_{1,2} \right| \\ &\leq \left| \mathbf{W}_{2,2} \sigma_{\text{ReLU}} \left\{ \mathbf{W}_{2,1} [\mathbf{x}_2^\top(\tau), \mathbf{x}'_2^\top(\tau), \mathbf{u}^\top(\tau)]^\top + \mathbf{b}_{2,1} \right\} - \mathbf{W}_{1,2} \sigma_{\text{ReLU}} \left\{ \mathbf{W}_{2,1} [\mathbf{x}_2^\top(\tau), \mathbf{x}'_2^\top(\tau), \mathbf{u}^\top(\tau)]^\top + \mathbf{b}_{2,1} \right\} \right. \\ &\quad \left. + \mathbf{W}_{1,2} \sigma_{\text{ReLU}} \left\{ \mathbf{W}_{2,1} [\mathbf{x}_2^\top(\tau), \mathbf{x}'_2^\top(\tau), \mathbf{u}^\top(\tau)]^\top + \mathbf{b}_{2,1} \right\} - \mathbf{W}_{1,2} \sigma_{\text{ReLU}} \left\{ \mathbf{W}_{1,1} [\mathbf{x}_2^\top(\tau), \mathbf{x}'_2^\top(\tau), \mathbf{u}^\top(\tau)]^\top + \mathbf{b}_{1,1} \right\} \right. \\ &\quad \left. + |\mathbf{b}_{2,2} - \mathbf{b}_{1,2}| \right| \\ &\leq w_{\Gamma, \text{out}} |\mathbf{W}_{2,2} - \mathbf{W}_{1,2}|_{\infty, \infty} \left| \sigma_{\text{ReLU}} \left\{ \mathbf{W}_{2,1} [\mathbf{x}_2^\top(\tau), \mathbf{x}'_2^\top(\tau), \mathbf{u}^\top(\tau)]^\top + \mathbf{b}_{2,1} \right\} \right| \\ &\quad + w_{\Gamma, \text{out}} |\mathbf{W}_{1,2}|_{\infty, \infty} \left| \left\{ \mathbf{W}_{2,1} [\mathbf{x}_2^\top(\tau), \mathbf{x}'_2^\top(\tau), \mathbf{u}^\top(\tau)]^\top + \mathbf{b}_{2,1} \right\} - \left\{ \mathbf{W}_{1,1} [\mathbf{x}_2^\top(\tau), \mathbf{x}'_2^\top(\tau), \mathbf{u}^\top(\tau)]^\top + \mathbf{b}_{1,1} \right\} \right| \\ &\quad + w_{\Gamma, \text{out}} |\mathbf{b}_{2,2} - \mathbf{b}_{1,2}|_{\infty} \\ &\leq \varsigma w_{\Gamma, \text{out}} \left| \mathbf{W}_{2,1} [\mathbf{x}_2^\top(\tau), \mathbf{x}'_2^\top(\tau), \mathbf{u}^\top(\tau)]^\top + \mathbf{b}_{2,1} \right| + \varsigma w_{\Gamma, \text{out}} \\ &\quad + w_{\Gamma, \text{out}} B_{\mathbf{W}} \left\{ \left| (\mathbf{W}_{2,1} - \mathbf{W}_{1,1}) [\mathbf{x}_2^\top(\tau), \mathbf{x}'_2^\top(\tau), \mathbf{u}^\top(\tau)]^\top \right| + |\mathbf{b}_{2,1} - \mathbf{b}_{1,1}| \right\} \\ &\stackrel{(a)}{\leq} \varsigma w_{\Gamma, \text{out}} \left(w_{\Gamma} B_{\mathbf{W}} \left\{ T [pB_K L_{\mathcal{F}_T} + w_{\Gamma, \text{out}} B_{\mathbf{b}} (w_{\Gamma} B_{\mathbf{W}} + 1)] e^{T(L_{\mathcal{F}_T} + 1)} + pB_K \right\} + w_{\Gamma} B_{\mathbf{b}} \right) \\ &\quad + w_{\Gamma, \text{out}} B_{\mathbf{W}} \left(w_{\Gamma} \varsigma \left\{ T [pB_K L_{\mathcal{F}_T} + w_{\Gamma, \text{out}} B_{\mathbf{b}} (w_{\Gamma} B_{\mathbf{W}} + 1)] e^{T(L_{\mathcal{F}_T} + 1)} + pB_K \right\} + w_{\Gamma} \varsigma \right) + \varsigma w_{\Gamma, \text{out}} \\ &\stackrel{(b)}{\leq} \varsigma w_{\Gamma, \text{out}} w_{\Gamma} \left(B_{\mathbf{W}} \left\{ T [pB_K (L_{\mathcal{F}_T} + 1) + w_{\Gamma, \text{out}} B_{\mathbf{b}} (w_{\Gamma} B_{\mathbf{W}} + 1)] e^{T(L_{\mathcal{F}_T} + 1)} \right\} + B_{\mathbf{b}} \right) \\ &\quad + w_{\Gamma, \text{out}} B_{\mathbf{W}} w_{\Gamma} \varsigma \left\{ \left\{ T [pB_K (L_{\mathcal{F}_T} + 1) + w_{\Gamma, \text{out}} B_{\mathbf{b}} (w_{\Gamma} B_{\mathbf{W}} + 1)] e^{T(L_{\mathcal{F}_T} + 1)} \right\} + 1 \right\} + \varsigma w_{\Gamma, \text{out}} \\ &\leq 2\varsigma w_{\Gamma, \text{out}} w_{\Gamma} \max(B_{\mathbf{W}}, B_{\mathbf{b}}) \left\{ T [pB_K (L_{\mathcal{F}_T} + 1) + w_{\Gamma, \text{out}} B_{\mathbf{b}} (w_{\Gamma} B_{\mathbf{W}} + 1)] e^{T(L_{\mathcal{F}_T} + 1)} + 1 \right\} + \varsigma w_{\Gamma, \text{out}} \\ &\stackrel{(c)}{\leq} 2\varsigma w_{\Gamma, \text{out}} w_{\Gamma} pT e^{T(L_{\mathcal{F}_T} + 1)} \{ \max(B_{\mathbf{W}}, B_{\mathbf{b}}) [B_K (L_{\mathcal{F}_T} + 1) + w_{\Gamma, \text{out}} B_{\mathbf{b}} (w_{\Gamma} B_{\mathbf{W}} + 1) + 1] + 1 \}, \end{aligned} \quad (\text{A.23})$$

where Step (a) utilizes Eq. (23) in Lemma 6 and Steps (b) and (c) hold from $T \geq 1$ in Assumption 1. Substituting Eq. (A.23) into Eq. (A.22), Eq. (24) is proven. \blacksquare

Appendix A.6. Proof of Lemma 8

Proof: $|II_1(\mathbf{x}) - II_2(\mathbf{x})|$ is bounded by

$$\begin{aligned}
|II_1(\mathbf{x}) - II_2(\mathbf{x})| &\leq \left| \tilde{\mathbf{W}}_{1,h_{II}} \sigma_{\text{ReLU}} \left[\dots \sigma_{\text{ReLU}} \left(\tilde{\mathbf{W}}_{1,1} \mathbf{x} + \tilde{\mathbf{b}}_{1,1} \right) \right] \right. \\
&\quad \left. - \tilde{\mathbf{W}}_{2,h_{II}} \sigma_{\text{ReLU}} \left[\dots \sigma_{\text{ReLU}} \left(\tilde{\mathbf{W}}_{2,1} \mathbf{x} + \tilde{\mathbf{b}}_{2,1} \right) \right] \right| + |\tilde{\mathbf{b}}_{1,h_{II}} - \tilde{\mathbf{b}}_{2,h_{II}}| \\
&\leq \left| \tilde{\mathbf{W}}_{1,h_{II}} \sigma_{\text{ReLU}} \left[\dots \sigma_{\text{ReLU}} \left(\tilde{\mathbf{W}}_{1,1} \mathbf{x} + \tilde{\mathbf{b}}_{1,1} \right) \right] - \tilde{\mathbf{W}}_{2,h_{II}} \sigma_{\text{ReLU}} \left[\dots \sigma_{\text{ReLU}} \left(\tilde{\mathbf{W}}_{1,1} \mathbf{x} + \tilde{\mathbf{b}}_{1,1} \right) \right] \right. \\
&\quad \left. + \tilde{\mathbf{W}}_{2,h_{II}} \sigma_{\text{ReLU}} \left[\dots \sigma_{\text{ReLU}} \left(\tilde{\mathbf{W}}_{1,1} \mathbf{x} + \tilde{\mathbf{b}}_{1,1} \right) \right] \right. \\
&\quad \left. - \tilde{\mathbf{W}}_{2,h_{II}} \sigma_{\text{ReLU}} \left[\dots \sigma_{\text{ReLU}} \left(\tilde{\mathbf{W}}_{2,1} \mathbf{x} + \tilde{\mathbf{b}}_{2,1} \right) \right] \right| + w_{II,\text{out}} \mathcal{S} \\
&\leq \left| \tilde{\mathbf{W}}_{1,h_{II}}^\top - \tilde{\mathbf{W}}_{2,h_{II}}^\top \right|_{\infty,1} \left| \sigma_{\text{ReLU}} \left[\dots \sigma_{\text{ReLU}} \left(\tilde{\mathbf{W}}_{1,1} \mathbf{x} + \tilde{\mathbf{b}}_{1,1} \right) \right] \right| + w_{II,\text{out}} \mathcal{S} \\
&\quad + L_{\mathcal{F}_{II},\text{layer}} \left| \sigma_{\text{ReLU}} \left[\dots \sigma_{\text{ReLU}} \left(\tilde{\mathbf{W}}_{1,1} \mathbf{x} + \tilde{\mathbf{b}}_{1,1} \right) \right] - \sigma_{\text{ReLU}} \left[\dots \sigma_{\text{ReLU}} \left(\tilde{\mathbf{W}}_{2,1} \mathbf{x} + \tilde{\mathbf{b}}_{2,1} \right) \right] \right|,
\end{aligned} \tag{A.24}$$

where $L_{\mathcal{F}_{II},\text{layer}} = \max_{j \in \{1,2,\dots,h_{II}\}} L_{\mathcal{F}_{II},j}$ and $L_{\mathcal{F}_{II},j}$ is an arbitrary L^1 -norm Lipschitz constant that bounds the mappings between the $(j-1)$ th and j th layers of all $II(\cdot) \in \mathcal{F}_{II}$, for $j = 1, 2, \dots, h_{II}$. $\left| \sigma_{\text{ReLU}} \left[\dots \sigma_{\text{ReLU}} \left(\tilde{\mathbf{W}}_{1,1} \mathbf{x} + \tilde{\mathbf{b}}_{1,1} \right) \right] \right|$ in Eq. (A.24) is bounded by

$$\begin{aligned}
\left| \sigma_{\text{ReLU}} \left[\dots \sigma_{\text{ReLU}} \left(\tilde{\mathbf{W}}_{1,1} \mathbf{x} + \tilde{\mathbf{b}}_{1,1} \right) \right] \right| &\leq L_{\mathcal{F}_{II},\text{layer}} \left| \sigma_{\text{ReLU}} \left[\dots \sigma_{\text{ReLU}} \left(\tilde{\mathbf{W}}_{1,1} \mathbf{x} + \tilde{\mathbf{b}}_{1,1} \right) \right] \right| + w_{II} B_{\tilde{\mathbf{b}}} \\
&\leq L_{\mathcal{F}_{II},\text{layer}}^2 \left| \sigma_{\text{ReLU}} \left[\dots \sigma_{\text{ReLU}} \left(\tilde{\mathbf{W}}_{1,1} \mathbf{x} + \tilde{\mathbf{b}}_{1,1} \right) \right] \right| + w_{II} B_{\tilde{\mathbf{b}}} (1 + L_{\mathcal{F}_{II},\text{layer}}) \\
&\leq L_{\mathcal{F}_{II},\text{layer}}^{h_{II}-1} |\mathbf{x}| + w_{II} B_{\tilde{\mathbf{b}}} \sum_{i=0}^{h_{II}-2} L_{\mathcal{F}_{II},\text{layer}}^i.
\end{aligned} \tag{A.25}$$

Substituting Eq. (A.25) into Eq. (A.24), $|II_1(\mathbf{x}) - II_2(\mathbf{x})|$ is bounded by

$$\begin{aligned}
&|II_1(\mathbf{x}) - II_2(\mathbf{x})| \\
&\leq w_{II,\text{out}} \mathcal{S} \left(L_{\mathcal{F}_{II},\text{layer}}^{h_{II}-1} |\mathbf{x}| + w_{II} B_{\tilde{\mathbf{b}}} \sum_{i=0}^{h_{II}-2} L_{\mathcal{F}_{II},\text{layer}}^i + 1 \right) \\
&\quad + L_{\mathcal{F}_{II},\text{layer}} \left| \tilde{\mathbf{W}}_{1,h_{II}-1} \sigma_{\text{ReLU}} \left[\dots \sigma_{\text{ReLU}} \left(\tilde{\mathbf{W}}_{1,1} \mathbf{x} + \tilde{\mathbf{b}}_{1,1} \right) \right] + \tilde{\mathbf{b}}_{1,h_{II}-1} - \tilde{\mathbf{W}}_{2,h_{II}-1} \sigma_{\text{ReLU}} \left[\dots \sigma_{\text{ReLU}} \left(\tilde{\mathbf{W}}_{2,1} \mathbf{x} + \tilde{\mathbf{b}}_{2,1} \right) \right] - \tilde{\mathbf{b}}_{2,h_{II}-1} \right|.
\end{aligned} \tag{A.26}$$

Similarly, the last term of Eq. (A.26) is bounded by

$$\begin{aligned}
&\left| \tilde{\mathbf{W}}_{1,h_{II}-1} \sigma_{\text{ReLU}} \left[\dots \sigma_{\text{ReLU}} \left(\tilde{\mathbf{W}}_{1,1} \mathbf{x} + \tilde{\mathbf{b}}_{1,1} \right) \right] + \tilde{\mathbf{b}}_{1,h_{II}-1} - \tilde{\mathbf{W}}_{2,h_{II}-1} \sigma_{\text{ReLU}} \left[\dots \sigma_{\text{ReLU}} \left(\tilde{\mathbf{W}}_{2,1} \mathbf{x} + \tilde{\mathbf{b}}_{2,1} \right) \right] - \tilde{\mathbf{b}}_{2,h_{II}-1} \right| \\
&\leq w_{II} \mathcal{S} \left(L_{\mathcal{F}_{II},\text{layer}}^{h_{II}-2} |\mathbf{x}| + w_{II} B_{\tilde{\mathbf{b}}} \sum_{i=0}^{h_{II}-3} L_{\mathcal{F}_{II},\text{layer}}^i + 1 \right) \\
&\quad + L_{\mathcal{F}_{II},\text{layer}} \left| \tilde{\mathbf{W}}_{1,h_{II}-2} \sigma_{\text{ReLU}} \left[\dots \sigma_{\text{ReLU}} \left(\tilde{\mathbf{W}}_{1,1} \mathbf{x} + \tilde{\mathbf{b}}_{1,1} \right) \right] + \tilde{\mathbf{b}}_{1,h_{II}-2} - \tilde{\mathbf{W}}_{2,h_{II}-2} \sigma_{\text{ReLU}} \left[\dots \sigma_{\text{ReLU}} \left(\tilde{\mathbf{W}}_{2,1} \mathbf{x} + \tilde{\mathbf{b}}_{2,1} \right) \right] - \tilde{\mathbf{b}}_{2,h_{II}-2} \right|.
\end{aligned} \tag{A.27}$$

By solving the iteration in Eq. (A.27), the last term of Eq. (A.26) is bounded by

$$\begin{aligned}
&\left| \tilde{\mathbf{W}}_{1,h_{II}-1} \sigma_{\text{ReLU}} \left[\dots \sigma_{\text{ReLU}} \left(\tilde{\mathbf{W}}_{1,1} \mathbf{x} + \tilde{\mathbf{b}}_{1,1} \right) \right] + \tilde{\mathbf{b}}_{1,h_{II}-1} - \tilde{\mathbf{W}}_{2,h_{II}-1} \sigma_{\text{ReLU}} \left[\dots \sigma_{\text{ReLU}} \left(\tilde{\mathbf{W}}_{2,1} \mathbf{x} + \tilde{\mathbf{b}}_{2,1} \right) \right] - \tilde{\mathbf{b}}_{2,h_{II}-1} \right| \\
&\leq w_{II} \mathcal{S} \left(L_{\mathcal{F}_{II},\text{layer}}^{h_{II}-2} |\mathbf{x}| + w_{II} B_{\tilde{\mathbf{b}}} \sum_{i=0}^{h_{II}-3} L_{\mathcal{F}_{II},\text{layer}}^i + 1 \right) + w_{II} \mathcal{S} L_{\mathcal{F}_{II},\text{layer}} \left(L_{\mathcal{F}_{II},\text{layer}}^{h_{II}-3} |\mathbf{x}| + w_{II} B_{\tilde{\mathbf{b}}} \sum_{i=0}^{h_{II}-4} L_{\mathcal{F}_{II},\text{layer}}^i + 1 \right) \\
&\quad + L_{\mathcal{F}_{II},\text{layer}}^2 \left| \tilde{\mathbf{W}}_{1,h_{II}-3} \sigma_{\text{ReLU}} \left[\dots \sigma_{\text{ReLU}} \left(\tilde{\mathbf{W}}_{1,1} \mathbf{x} + \tilde{\mathbf{b}}_{1,1} \right) \right] + \tilde{\mathbf{b}}_{1,h_{II}-3} - \tilde{\mathbf{W}}_{2,h_{II}-3} \sigma_{\text{ReLU}} \left[\dots \sigma_{\text{ReLU}} \left(\tilde{\mathbf{W}}_{2,1} \mathbf{x} + \tilde{\mathbf{b}}_{2,1} \right) \right] - \tilde{\mathbf{b}}_{2,h_{II}-3} \right| \\
&\leq w_{II} \mathcal{S} \sum_{j=0}^{h_{II}-3} L_{\mathcal{F}_{II},\text{layer}}^j \left(L_{\mathcal{F}_{II},\text{layer}}^{h_{II}-2-j} |\mathbf{x}| + w_{II} B_{\tilde{\mathbf{b}}} \sum_{i=0}^{h_{II}-3-j} L_{\mathcal{F}_{II},\text{layer}}^i + 1 \right) + L_{\mathcal{F}_{II},\text{layer}}^{h_{II}-2} \left| \left(\tilde{\mathbf{W}}_{1,1} \mathbf{x} + \tilde{\mathbf{b}}_{1,1} \right) - \left(\tilde{\mathbf{W}}_{2,1} \mathbf{x} + \tilde{\mathbf{b}}_{2,1} \right) \right| \\
&\leq w_{II} \mathcal{S} \sum_{j=0}^{h_{II}-3} L_{\mathcal{F}_{II},\text{layer}}^j \left(L_{\mathcal{F}_{II},\text{layer}}^{h_{II}-2-j} |\mathbf{x}| + w_{II} B_{\tilde{\mathbf{b}}} \frac{1-L_{\mathcal{F}_{II},\text{layer}}^{h_{II}-2-j}}{1-L_{\mathcal{F}_{II},\text{layer}}} + 1 \right) + L_{\mathcal{F}_{II},\text{layer}}^{h_{II}-2} w_{II} \mathcal{S} (|\mathbf{x}| + 1) \\
&= w_{II} \mathcal{S} \sum_{i=0}^{h_{II}-2} L_{\mathcal{F}_{II},\text{layer}}^i \left(L_{\mathcal{F}_{II},\text{layer}}^{h_{II}-2-i} |\mathbf{x}| + w_{II} B_{\tilde{\mathbf{b}}} \frac{1-L_{\mathcal{F}_{II},\text{layer}}^{h_{II}-2-i}}{1-L_{\mathcal{F}_{II},\text{layer}}} + 1 \right).
\end{aligned} \tag{A.28}$$

Substituting Eq. (A.28) into Eq. (A.26), $|\Pi_1(\mathbf{x}) - \Pi_2(\mathbf{x})|$ is bounded by

$$\begin{aligned}
|\Pi_1(\mathbf{x}) - \Pi_2(\mathbf{x})| &\leq w_{\Pi, \text{out}} \mathcal{S} \left(L_{\mathcal{F}_{\Pi}, \text{layer}}^{h_{\Pi}-1} |\mathbf{x}| + w_{\Pi} B_{\mathbf{b}} \sum_{i=0}^{h_{\Pi}-2} L_{\mathcal{F}_{\Pi}, \text{layer}}^i + 1 \right) \\
&\quad + L_{\mathcal{F}_{\Pi}, \text{layer}} w_{\Pi} \mathcal{S} \sum_{i=0}^{h_{\Pi}-2} L_{\mathcal{F}_{\Pi}, \text{layer}}^i \left(L_{\mathcal{F}_{\Pi}, \text{layer}}^{h_{\Pi}-2-i} |\mathbf{x}| + w_{\Pi} B_{\mathbf{b}} \frac{1-L_{\mathcal{F}_{\Pi}, \text{layer}}^{h_{\Pi}-2-i}}{1-L_{\mathcal{F}_{\Pi}, \text{layer}}} + 1 \right) \\
&= w_{\Pi, \text{out}} \mathcal{S} \left(L_{\mathcal{F}_{\Pi}, \text{layer}}^{h_{\Pi}-1} |\mathbf{x}| + w_{\Pi} B_{\mathbf{b}} \sum_{i=0}^{h_{\Pi}-2} L_{\mathcal{F}_{\Pi}, \text{layer}}^i + 1 \right) \\
&\quad + w_{\Pi} \mathcal{S} \sum_{i=1}^{h_{\Pi}-1} L_{\mathcal{F}_{\Pi}, \text{layer}}^i \left(L_{\mathcal{F}_{\Pi}, \text{layer}}^{h_{\Pi}-1-i} |\mathbf{x}| + w_{\Pi} B_{\mathbf{b}} \frac{1-L_{\mathcal{F}_{\Pi}, \text{layer}}^{h_{\Pi}-1-i}}{1-L_{\mathcal{F}_{\Pi}, \text{layer}}} + 1 \right) \\
&\leq \max(w_{\Gamma, \text{out}}, w_{\Gamma}) \mathcal{S} \sum_{i=0}^{h_{\Pi}-1} L_{\mathcal{F}_{\Pi}, \text{layer}}^i \left(L_{\mathcal{F}_{\Pi}, \text{layer}}^{h_{\Pi}-1-i} |\mathbf{x}| + w_{\Pi} B_{\mathbf{b}} \frac{1-L_{\mathcal{F}_{\Pi}, \text{layer}}^{h_{\Pi}-1-i}}{1-L_{\mathcal{F}_{\Pi}, \text{layer}}} + 1 \right) \\
&= \max(w_{\Gamma, \text{out}}, w_{\Gamma}) \mathcal{S} \left(h_{\Pi} L_{\mathcal{F}_{\Pi}, \text{layer}}^{h_{\Pi}-1} |\mathbf{x}| + \sum_{i=0}^{h_{\Pi}-1} L_{\mathcal{F}_{\Pi}, \text{layer}}^i + w_{\Pi} B_{\mathbf{b}} \sum_{i=0}^{h_{\Pi}-2} \sum_{j=i}^{h_{\Pi}-2} L_{\mathcal{F}_{\Pi}, \text{layer}}^j \right) \\
&\leq \varsigma \max(w_{\Gamma, \text{out}}, w_{\Gamma}) h_{\Pi}^2 \left(L_{\mathcal{F}_{\Pi}, \text{layer}}^{h_{\Pi}-1} + 1 \right) (|\mathbf{x}| + w_{\Pi} B_{\mathbf{b}} + 1).
\end{aligned} \tag{A.29}$$

This completes the proof. \blacksquare

Appendix A.7. Proof of Lemma 9

Proof: $|\Pi_1 \circ \Phi_{\Gamma_1}[\mathbf{u}(\tau)](t) - \Pi_2 \circ \Phi_{\Gamma_2}[\mathbf{u}(\tau)](t)|$ is bounded by

$$\begin{aligned}
&|\Pi_1 \circ \Phi_{\Gamma_1}[\mathbf{u}(\tau)](t) - \Pi_2 \circ \Phi_{\Gamma_2}[\mathbf{u}(\tau)](t)| \\
&\leq |\Pi_1 \circ \Phi_{\Gamma_1}[\mathbf{u}(\tau)](t) - \Pi_1 \circ \Phi_{\Gamma_2}[\mathbf{u}(\tau)](t)| + |\Pi_1 \circ \Phi_{\Gamma_2}[\mathbf{u}(\tau)](t) - \Pi_2 \circ \Phi_{\Gamma_2}[\mathbf{u}(\tau)](t)|.
\end{aligned} \tag{A.30}$$

From Lemma 7, $|\Pi_1 \circ \Phi_{\Gamma_1}[\mathbf{u}(\tau)](t) - \Pi_1 \circ \Phi_{\Gamma_2}[\mathbf{u}(\tau)](t)|$ in Eq. (A.30) is bounded by

$$\begin{aligned}
&|\Pi_1 \circ \Phi_{\Gamma_1}[\mathbf{u}(\tau)](t) - \Pi_1 \circ \Phi_{\Gamma_2}[\mathbf{u}(\tau)](t)| \\
&\leq 2L_{\mathcal{F}_{\Pi}} \varsigma w_{\Gamma, \text{out}} w_{\Gamma} p T^2 e^{2T(L_{\mathcal{F}_{\Gamma}}+1)} \{ \max(B_{\mathbf{W}}, B_{\mathbf{b}}) [B_K(L_{\mathcal{F}_{\Gamma}}+1) + w_{\Gamma, \text{out}} B_{\mathbf{b}} (w_{\Gamma} B_{\mathbf{W}} + 1) + 1] + 1 \},
\end{aligned} \tag{A.31}$$

where $L_{\mathcal{F}_{\Pi}}$ is an arbitrary L^1 -norm Lipschitz constant for all $\Pi(\cdot) \in \mathcal{F}_{\Pi}$. From Eq. (1), Lemma 6, and Lemma 8, $|\Pi_1 \circ \Phi_{\Gamma_2}[\mathbf{u}(\tau)](t) - \Pi_2 \circ \Phi_{\Gamma_2}[\mathbf{u}(\tau)](t)|$ in Eq. (A.30) with $\mathbf{x}(t) = \Phi_{\Gamma_2}[\mathbf{u}(\tau)](t)$ is bounded by

$$\begin{aligned}
&|\Pi_1 \circ \Phi_{\Gamma_2}[\mathbf{u}(\tau)](t) - \Pi_2 \circ \Phi_{\Gamma_2}[\mathbf{u}(\tau)](t)| \\
&\leq \varsigma \max(w_{\Gamma, \text{out}}, w_{\Gamma}) h_{\Pi}^2 \left(L_{\mathcal{F}_{\Pi}, \text{layer}}^{h_{\Pi}-1} + 1 \right) (|\mathbf{x}(t)| + |\mathbf{u}_0| + t + w_{\Pi} B_{\mathbf{b}} + 1) \\
&\leq \varsigma \max(w_{\Gamma, \text{out}}, w_{\Gamma}) h_{\Pi}^2 \left(L_{\mathcal{F}_{\Pi}, \text{layer}}^{h_{\Pi}-1} + 1 \right) \left\{ T [pB_K L_{\mathcal{F}_{\Gamma}} + w_{\Gamma, \text{out}} B_{\mathbf{b}} (w_{\Gamma} B_{\mathbf{W}} + 1)] e^{T(L_{\mathcal{F}_{\Gamma}}+1)} + pB_K + T + w_{\Pi} B_{\mathbf{b}} + 1 \right\} \\
&\leq \varsigma \max(w_{\Gamma, \text{out}}, w_{\Gamma}) h_{\Pi}^2 \left(L_{\mathcal{F}_{\Pi}, \text{layer}}^{h_{\Pi}-1} + 1 \right) T [pB_K (L_{\mathcal{F}_{\Gamma}} + 1) + w_{\Gamma, \text{out}} B_{\mathbf{b}} (w_{\Gamma} B_{\mathbf{W}} + 1) + w_{\Pi} B_{\mathbf{b}} + 2] e^{T(L_{\mathcal{F}_{\Gamma}}+1)} \\
&\leq \varsigma \max(w_{\Gamma, \text{out}}, w_{\Gamma}) h_{\Pi}^2 \left(L_{\mathcal{F}_{\Pi}, \text{layer}}^{h_{\Pi}-1} + 1 \right) p T e^{T(L_{\mathcal{F}_{\Gamma}}+1)} [B_K (L_{\mathcal{F}_{\Gamma}} + 1) + w_{\Gamma, \text{out}} B_{\mathbf{b}} (w_{\Gamma} B_{\mathbf{W}} + 1) + w_{\Pi} B_{\mathbf{b}} + 2].
\end{aligned} \tag{A.32}$$

Substituting Eqs. (A.31) and (A.32) into Eq. (A.30), $|\Pi_1 \circ \Phi_{\Gamma_1}[\mathbf{u}(\tau)](t) - \Pi_2 \circ \Phi_{\Gamma_2}[\mathbf{u}(\tau)](t)|$ can be bounded by

$$\begin{aligned}
&|\Pi_1 \circ \Phi_{\Gamma_1}[\mathbf{u}(\tau)](t) - \Pi_2 \circ \Phi_{\Gamma_2}[\mathbf{u}(\tau)](t)| \\
&\leq 2L_{\mathcal{F}_{\Pi}} \varsigma w_{\Gamma, \text{out}} w_{\Gamma} p T^2 e^{2T(L_{\mathcal{F}_{\Gamma}}+1)} \{ \max(B_{\mathbf{W}}, B_{\mathbf{b}}) [B_K (L_{\mathcal{F}_{\Gamma}} + 1) + w_{\Gamma, \text{out}} B_{\mathbf{b}} (w_{\Gamma} B_{\mathbf{W}} + 1) + 1] + 1 \} \\
&\quad + \varsigma \max(w_{\Gamma, \text{out}}, w_{\Gamma}) h_{\Pi}^2 \left(L_{\mathcal{F}_{\Pi}, \text{layer}}^{h_{\Pi}-1} + 1 \right) p T e^{T(L_{\mathcal{F}_{\Gamma}}+1)} [B_K (L_{\mathcal{F}_{\Gamma}} + 1) + w_{\Gamma, \text{out}} B_{\mathbf{b}} (w_{\Gamma} B_{\mathbf{W}} + 1) + w_{\Pi} B_{\mathbf{b}} + 2] \\
&\leq 3\varsigma \left(L_{\mathcal{F}_{\Pi}, \text{layer}}^{h_{\Pi}} + 1 \right) w_{\Pi} w_{\Gamma, \text{out}}^2 h_{\Pi}^2 p T^2 e^{2T(L_{\mathcal{F}_{\Gamma}}+1)} (L_{\mathcal{F}_{\Gamma}} + 1) B_K \{ [\max(B_{\mathbf{W}}, B_{\mathbf{b}}) + 1] [B_{\mathbf{b}} (B_{\mathbf{W}} + 1) + 2] + B_{\mathbf{b}} + 2 \}.
\end{aligned} \tag{A.33}$$

This completes the proof. \blacksquare

Appendix A.8. Proof of Lemma 10

Proof: Under Assumptions 1, 2, 8, 9, and 10, given MLPs $\Gamma_1(\cdot)$ and $\Gamma_2(\cdot) \in \mathcal{F}_{\Gamma}$ and MPLs $\Pi_1(\cdot)$ and $\Pi_2(\cdot) \in \mathcal{F}_{\Pi}$, the differences between the weight matrices and vectors of $\Gamma_1(\cdot)$ and $\Gamma_2(\cdot)$ and those of $\Pi_1(\cdot)$ and $\Pi_2(\cdot)$ are bounded

by ς , then, from Eq. (19) in Lemma 4 and Eq. (26) in Lemma 9, the pseudo-metric $d_\kappa(\Pi_1 \circ \Phi_{\Gamma_1}, \Pi_2 \circ \Phi_{\Gamma_2})$ between $\Pi_1 \circ \Phi_{\Gamma_1}$ and $\Pi_2 \circ \Phi_{\Gamma_2} \in \mathcal{F}_{\Pi \circ \Phi_\Gamma}$, is bounded by

$$\begin{aligned} d_\kappa(\Pi_1 \circ \Phi_{\Gamma_1}, \Pi_2 \circ \Phi_{\Gamma_2}) &= \sqrt{\sum_{i=1}^N \left\| \Pi_1 \circ \Phi_{\Gamma_1} [\mathbf{u}_i(\tau)](t) - \Pi_2 \circ \Phi_{\Gamma_2} [\mathbf{u}_i(\tau)](t) \right\|_{L^2}^2} \\ &\leq \sqrt{TN} \max_{t \in [0, T]} \left| \Pi_1 \circ \Phi_{\Gamma_1} [\mathbf{u}(\tau)](t) - \Pi_2 \circ \Phi_{\Gamma_2} [\mathbf{u}(\tau)](t) \right| \leq \varsigma \sqrt{NT w_{\Pi, \text{out}} B_{\Pi} \Delta_{\Pi \circ \Phi_\Gamma}}, \end{aligned} \quad (\text{A.34})$$

where $\Delta_{\Pi \circ \Phi_\Gamma}$ is in Eq. (29).

For all neural oscillators $\Pi \circ \Phi_\Gamma \in \mathcal{F}_{\Pi \circ \Phi_\Gamma}$ in Assumption 10, the number $N_{\mathbf{W}}$ of the total tunable parameters in the weight matrices of an arbitrary $\Gamma(\cdot) \in \mathcal{F}_\Gamma$ is $N_{\mathbf{W}} = w_\Gamma (3w_{\Gamma, \text{out}} + p)$, the number $N_{\mathbf{b}}$ of the total tunable parameters in the weight vectors of $\Gamma(\cdot) \in \mathcal{F}_\Gamma$ is $N_{\mathbf{b}} = w_{\Gamma, \text{out}} + w_\Gamma$, the number $N_{\tilde{\mathbf{W}}}$ of the total tunable parameters in the weight matrices of an arbitrary $\Pi(\cdot) \in \mathcal{F}_\Pi$ is $N_{\tilde{\mathbf{W}}} = w_\Pi^2 (h_\Pi - 2) + w_\Pi (w_{\Gamma, \text{out}} + p + w_{\Pi, \text{out}} + 1)$, and the number $N_{\tilde{\mathbf{b}}}$ of the total tunable parameters in the weight vectors of $\Pi(\cdot) \in \mathcal{F}_\Pi$ is $N_{\tilde{\mathbf{b}}} = w_{\Pi, \text{out}} + (h_\Pi - 1)w_\Pi$. By discretizing the range of values for each weight parameter using a uniform grid with a grid size of ς , the number of the obtained neural oscillators is

$$\left(\frac{2B_{\mathbf{W}}}{\varsigma} \right)^{N_{\mathbf{W}}} \left(\frac{2B_{\mathbf{b}}}{\varsigma} \right)^{N_{\mathbf{b}}} \left(\frac{2B_{\tilde{\mathbf{W}}}}{\varsigma} \right)^{N_{\tilde{\mathbf{W}}}} \left(\frac{2B_{\tilde{\mathbf{b}}}}{\varsigma} \right)^{N_{\tilde{\mathbf{b}}}}. \quad (\text{A.35})$$

Based on Eq. (A.34), these neural oscillators cover the neural oscillator class $\mathcal{F}_{\Pi \circ \Phi_\Gamma}$ by a distance $\varepsilon = \varsigma \sqrt{NT w_{\Pi, \text{out}} B_{\Pi} \Delta_{\Pi \circ \Phi_\Gamma}}$. Thus, the covering number $N(\mathcal{F}_{\Pi \circ \Phi_\Gamma}, d_\kappa, \varepsilon)$ can be bounded by

$$N(\mathcal{F}_{\Pi \circ \Phi_\Gamma}, d_\kappa, \varepsilon) \leq \left(\frac{B_{\mathbf{W}} \sqrt{NT w_{\Pi, \text{out}} B_{\Pi} \Delta_{\Pi \circ \Phi_\Gamma}}}{0.5\varepsilon} \right)^{N_{\mathbf{W}}} \left(\frac{B_{\mathbf{b}} \sqrt{NT w_{\Pi, \text{out}} B_{\Pi} \Delta_{\Pi \circ \Phi_\Gamma}}}{0.5\varepsilon} \right)^{N_{\mathbf{b}}} \left(\frac{B_{\tilde{\mathbf{W}}} \sqrt{NT w_{\Pi, \text{out}} B_{\Pi} \Delta_{\Pi \circ \Phi_\Gamma}}}{0.5\varepsilon} \right)^{N_{\tilde{\mathbf{W}}}} \left(\frac{B_{\tilde{\mathbf{b}}} \sqrt{NT w_{\Pi, \text{out}} B_{\Pi} \Delta_{\Pi \circ \Phi_\Gamma}}}{0.5\varepsilon} \right)^{N_{\tilde{\mathbf{b}}}}. \quad (\text{A.36})$$

Given an inequality

$$\int_0^b \sqrt{\ln\left(\frac{a}{\varepsilon}\right)} d\varepsilon \leq \int_0^b \sqrt{\ln\left(1 + \frac{a}{\varepsilon}\right)} d\varepsilon = a \int_0^{b/a} \sqrt{\ln\left(1 + \frac{1}{\varepsilon}\right)} d\varepsilon \stackrel{(a)}{\leq} b \sqrt{\ln\left[3\left(1 + \frac{a}{b}\right)\right]}, \quad (\text{A.37})$$

where Step (a) is from Lemma C.9 of Foucart and Rauhut (2013). The integral in Eq. (22) is bounded by

$$\begin{aligned} &\int_0^{\sqrt{NT w_{\Pi, \text{out}} B_{\Pi}}} \sqrt{\ln N(\mathcal{F}_{\Pi \circ \Phi_\Gamma}, d_\kappa, \varepsilon)} d\varepsilon \\ &\leq \int_0^{\sqrt{NT w_{\Pi, \text{out}} B_{\Pi}}} \sqrt{N_{\mathbf{W}} \ln\left(\frac{B_{\mathbf{W}} \sqrt{NT w_{\Pi, \text{out}} B_{\Pi} \Delta_{\Pi \circ \Phi_\Gamma}}}{0.5\varepsilon}\right)} d\varepsilon + \int_0^{\sqrt{NT w_{\Pi, \text{out}} B_{\Pi}}} \sqrt{N_{\mathbf{b}} \ln\left(\frac{B_{\mathbf{b}} \sqrt{NT w_{\Pi, \text{out}} B_{\Pi} \Delta_{\Pi \circ \Phi_\Gamma}}}{0.5\varepsilon}\right)} d\varepsilon \\ &\quad + \int_0^{\sqrt{NT w_{\Pi, \text{out}} B_{\Pi}}} \sqrt{N_{\tilde{\mathbf{W}}} \ln\left(\frac{B_{\tilde{\mathbf{W}}} \sqrt{NT w_{\Pi, \text{out}} B_{\Pi} \Delta_{\Pi \circ \Phi_\Gamma}}}{0.5\varepsilon}\right)} d\varepsilon + \int_0^{\sqrt{NT w_{\Pi, \text{out}} B_{\Pi}}} \sqrt{N_{\tilde{\mathbf{b}}} \ln\left(\frac{B_{\tilde{\mathbf{b}}} \sqrt{NT w_{\Pi, \text{out}} B_{\Pi} \Delta_{\Pi \circ \Phi_\Gamma}}}{0.5\varepsilon}\right)} d\varepsilon \\ &\leq \sqrt{NT w_{\Pi, \text{out}} B_{\Pi}} \sqrt{w_\Gamma (3w_{\Gamma, \text{out}} + p) \ln(3 + 6B_{\mathbf{W}} \Delta_{\Pi \circ \Phi_\Gamma})} \\ &\quad + \sqrt{NT w_{\Pi, \text{out}} B_{\Pi}} \sqrt{(w_{\Gamma, \text{out}} + w_\Gamma) \ln(3 + 6B_{\mathbf{b}} \Delta_{\Pi \circ \Phi_\Gamma})} \\ &\quad + \sqrt{NT w_{\Pi, \text{out}} B_{\Pi}} \sqrt{\left[w_\Pi^2 (h_\Pi - 2) + w_\Pi (w_{\Gamma, \text{out}} + p + w_{\Pi, \text{out}} + 1) \right] \ln(3 + 6B_{\tilde{\mathbf{W}}} \Delta_{\Pi \circ \Phi_\Gamma})} \\ &\quad + \sqrt{NT w_{\Pi, \text{out}} B_{\Pi}} \sqrt{[w_{\Pi, \text{out}} + (h_\Pi - 1)w_\Pi] \ln(3 + 6B_{\tilde{\mathbf{b}}} \Delta_{\Pi \circ \Phi_\Gamma})}. \end{aligned} \quad (\text{A.38})$$

Substituting Eq. (A.38) into Eq. (22), Eq. (28) is proven. \blacksquare

Appendix A.9. Proof of Theorem 1

Proof: Under Assumptions 1-11, together with the conditions and results in Lemma 1, for the target causal and uniformly continuous operator Φ , with the specified sizes of $\Gamma(\cdot)$ and $\Pi(\cdot)$ from Lemma 1, the generalization error $\ell(\hat{\Pi} \circ \Phi_\Gamma)$ of a neural oscillator $\hat{\Pi} \circ \Phi_\Gamma$, learned by Eq. (12) with N i.i.d. sample pairs $\mathbf{U}_N(t)$ and $\mathbf{V}_N(t)$ from $\mu(\cdot)$, is bounded by Eq. (21) with probability at least $1 - \delta$ for $\forall \delta \in (0, 1)$. The empirical loss $\hat{\ell}_{\mathbf{U}_N, \mathbf{V}_N}(\hat{\Pi} \circ \Phi_\Gamma)$ in Eq. (21) can be bounded by $T\varepsilon_y^2$ with ε_y in Eq. (6) of Lemma 1. The empirical Rademacher complexity $\mathfrak{R}_{\mathcal{G}_\phi}$ in Eq. (21) can be bounded by the expected supremum $\kappa(\Pi \circ \Phi_\Gamma, \tilde{\sigma})$, as demonstrated in Lemma 3. By bounding the expected supremum of $\kappa(\Pi \circ \Phi_\Gamma, \tilde{\sigma})$ using Eq. (28) in Lemma 10, together with $w_{\Pi, \text{out}} = q$, $L_{\mathcal{F}_\Gamma} = w_{\max}^2 B_{\max}^2$, and $L_{\mathcal{F}_\Pi, \text{layer}}^{h_\Pi} = w_{\max}^{h_\Pi} B_{\max}^{h_\Pi}$ from Lemma 5, Eq. (30) is proven. \blacksquare

Appendix A.10. Proof of Theorem 2

Proof: Under Assumptions 1-11 and the conditions in Lemma 2, for the target second-order differential system governed by Eq. (7), with the specified sizes of $\Gamma(\cdot)$ and $\Pi(\cdot)$ from Lemma 2, by replacing the ε_γ in Eq. (30) with the bound $L_h B_{\beta_g} \sqrt{r} \varepsilon_1 + q \varepsilon_2$ in Eq. (8) of Lemma 2, the generalization error $\ell(\hat{\Pi} \circ \Phi_{\hat{r}})$ of $\hat{\Pi} \circ \Phi_{\hat{r}}$ learned by Eq. (12) with N i.i.d. sample pairs $\mathbf{U}_N(t)$ and $\mathbf{V}_N(t)$ from $\mu(\cdot)$ can be bounded by

$$\begin{aligned} \ell(\hat{\Pi} \circ \Phi_{\hat{r}}) &\leq T(L_h B_{\beta_g} \sqrt{r} \varepsilon_1 + q \varepsilon_2)^2 + 3 \frac{TqB_{\text{loss}}^2}{\sqrt{N}} \left[172w_{\text{max}}^{1.5} \sqrt{\ln(3 + 6B_{\text{max}} \Delta_{\Pi \circ \Phi_r})} + \sqrt{0.5 \log(2\delta^{-1})} \right] \\ &\leq 2T(L_h^2 B_{\beta_g}^2 r \varepsilon_1^2 + q^2 \varepsilon_2^2) + 3 \frac{TqB_{\text{loss}}^2}{\sqrt{N}} \left[172w_{\text{max}}^{1.5} \sqrt{\ln(3 + 6B_{\text{max}} \Delta_{\Pi \circ \Phi_r})} + \sqrt{0.5 \log(2\delta^{-1})} \right] \end{aligned} \quad (\text{A.39})$$

with probability at least $1 - \delta$ for $\forall \delta \in (0, 1)$, $\forall 0 < \varepsilon_1 < \alpha/r$, and $\forall \varepsilon_2 > 0$, where $\Delta_{\Pi \circ \Phi_r}$ is in Eq. (29) with $h_{\Pi} = 2$, $L_{\mathcal{F}_r} = w_{\text{max}}^2 B_{\text{max}}^2$, and $L_{\mathcal{F}_{\Pi, \text{layer}}}^{h_{\Pi}} = w_{\text{max}}^2 B_{\text{max}}^2$. From $w_r = 8r[C_r \varepsilon_1^{-2}]$, $w_{\Pi} = 8q[C_{\Pi} \varepsilon_2^{-2}]$, $w_{r, \text{out}} = r$, and $w_{\Pi, \text{out}} = q$ in Lemma 2, ε_1^2 and ε_2^2 can be replaced using w_r , and w_{Π} , respectively, thus obtaining Eq. (31). \blacksquare

Appendix B. Proof of Eq. (22)

Given an arbitrary integer M , let \mathcal{B}_m , $m = 1, 2, \dots, M$, be the subsets of $\mathcal{F}_{\Pi \circ \Phi_r}$, that each \mathcal{B}_m corresponds to a minimal $2\sqrt{NTw_{\Pi, \text{out}}} B_{\Pi} 2^{-m}$ -cover of $\mathcal{F}_{\Pi \circ \Phi_r}$, with the covering number $N(\mathcal{F}_{\Pi \circ \Phi_r}, d_k, 2\sqrt{NTw_{\Pi, \text{out}}} B_{\Pi} 2^{-m})$, where $2\sqrt{NTw_{\Pi, \text{out}}} B_{\Pi}$ is the bound of the diameter of $\mathcal{F}_{\Pi \circ \Phi_r}$, as shown in Eq. (20). Then, given $\forall \Pi \circ \Phi_r \in \mathcal{F}_{\Pi \circ \Phi_r}$, it can be expressed as

$$\kappa(\Pi \circ \Phi_r, \tilde{\sigma}) = \kappa(\Pi \circ \Phi_r, \tilde{\sigma}) - \kappa(\Pi_M \circ \Phi_{r_M}, \tilde{\sigma}) + \sum_{m=1}^M \kappa(\Pi_m \circ \Phi_{r_m}, \tilde{\sigma}) - \kappa(\Pi_{m-1} \circ \Phi_{r_{m-1}}, \tilde{\sigma}), \quad (\text{B.1})$$

where $\Pi_{m-1} \circ \Phi_{r_{m-1}} \in \mathcal{B}_{m-1}$ is closet to $\Pi_m \circ \Phi_{r_m}$, $m = 2, 3, \dots, M$, $\Pi_M \circ \Phi_{r_M} \in \mathcal{B}_M$ is closet to $\Pi \circ \Phi_r$, $\kappa(\Pi_0 \circ \Phi_{r_0}, \tilde{\sigma}) = 0$, and $\Pi_0 \circ \Phi_{r_0}$ represents case where the parameter of the MLPs $\Gamma(\cdot)$ and $\Pi(\cdot)$ are all zeros. $\kappa(\Pi \circ \Phi_r, \tilde{\sigma})$ can be bounded by

$$\begin{aligned} \kappa(\Pi \circ \Phi_r, \tilde{\sigma}) &\leq \sup_{\substack{d_k(\Pi_1 \circ \Phi_{r_1}, \Pi_2 \circ \Phi_{r_2}) \leq 2\sqrt{NTw_{\Pi, \text{out}}} B_{\Pi} 2^{-M} \\ \Pi_1 \circ \Phi_{r_1}, \Pi_2 \circ \Phi_{r_2} \in \mathcal{F}_{\Pi \circ \Phi_r}}} \kappa(\Pi_1 \circ \Phi_{r_1}, \tilde{\sigma}) - \kappa(\Pi_2 \circ \Phi_{r_2}, \tilde{\sigma}) \\ &\quad + \sum_{m=1}^M \sup_{\Pi_m \circ \Phi_{r_m} \in \mathcal{B}_m} \{\kappa(\Pi_m \circ \Phi_{r_m}, \tilde{\sigma}) - \kappa[\Pi_{m-1} \circ \Phi_{r_{m-1}}(\Pi_m \circ \Phi_{r_m}), \tilde{\sigma}]\} \end{aligned} \quad (\text{B.2})$$

and its expected supremum is bounded by

$$\begin{aligned} \mathbb{E}_{\tilde{\sigma}} \kappa(\Pi \circ \Phi_r, \tilde{\sigma}) &\leq \mathbb{E}_{\tilde{\sigma}} \sup_{\substack{d_k(\Pi_1 \circ \Phi_{r_1}, \Pi_2 \circ \Phi_{r_2}) \leq 2\sqrt{NTw_{\Pi, \text{out}}} B_{\Pi} 2^{-M} \\ \Pi_1 \circ \Phi_{r_1}, \Pi_2 \circ \Phi_{r_2} \in \mathcal{F}_{\Pi \circ \Phi_r}}} \kappa(\Pi_1 \circ \Phi_{r_1}, \tilde{\sigma}) - \kappa(\Pi_2 \circ \Phi_{r_2}, \tilde{\sigma}) \\ &\quad + \sum_{m=1}^M \mathbb{E}_{\tilde{\sigma}} \sup_{\Pi_m \circ \Phi_{r_m} \in \mathcal{B}_m} \{\kappa(\Pi_m \circ \Phi_{r_m}, \tilde{\sigma}) - \kappa[\Pi_{m-1} \circ \Phi_{r_{m-1}}(\Pi_m \circ \Phi_{r_m}), \tilde{\sigma}]\}. \end{aligned} \quad (\text{B.3})$$

Since the cardinalities of the subsets \mathcal{B}_m are finite, and the expected supremum of a sub-Gaussian process' increment over a finite index set can be bounded by the index's finite cardinality, as shown in the lemma on Page 2 of Bartlett (2013), the last term in Eq. (B.3) can be bounded by

$$\begin{aligned} &\sum_{m=1}^M \mathbb{E}_{\tilde{\sigma}} \sup_{\Pi_m \circ \Phi_{r_m} \in \mathcal{B}_m} \{\kappa(\Pi_m \circ \Phi_{r_m}, \tilde{\sigma}) - \kappa[\Pi_{m-1} \circ \Phi_{r_{m-1}}(\Pi_m \circ \Phi_{r_m}), \tilde{\sigma}]\} \\ &\leq \sum_{m=1}^M 2\sqrt{NTw_{\Pi, \text{out}}} B_{\Pi} 2^{-(m-1)} \sqrt{2 \ln N(\mathcal{F}_{\Pi \circ \Phi_r}, d_k, 2\sqrt{NTw_{\Pi, \text{out}}} B_{\Pi} 2^{-m})} \\ &= 4 \sum_{m=1}^M 2\sqrt{NTw_{\Pi, \text{out}}} B_{\Pi} 2^{-(m+1)} \sqrt{2 \ln N(\mathcal{F}_{\Pi \circ \Phi_r}, d_k, 2\sqrt{NTw_{\Pi, \text{out}}} B_{\Pi} 2^{-m})} \\ &\leq 4 \sum_{m=1}^M \int_2^{\sqrt{NTw_{\Pi, \text{out}}} B_{\Pi} 2^{-m}} \sqrt{2 \ln N(\mathcal{F}_{\Pi \circ \Phi_r}, d_k, \varepsilon)} d\varepsilon \\ &= 4\sqrt{2} \int_{\sqrt{NTw_{\Pi, \text{out}}} B_{\Pi} 2^{-M}}^{\sqrt{NTw_{\Pi, \text{out}}} B_{\Pi}} \sqrt{\ln N(\mathcal{F}_{\Pi \circ \Phi_r}, d_k, \varepsilon)} d\varepsilon. \end{aligned} \quad (\text{B.4})$$

Substituting Eq. (B.4) into Eq. (B.3), it can be obtained

$$\begin{aligned} \mathbb{E}_{\tilde{\sigma}} \kappa(\Pi \circ \Phi_{\Gamma}, \tilde{\sigma}) &\leq \mathbb{E}_{\tilde{\sigma}} \sup_{\substack{d_k(\Pi_1 \circ \Phi_{\Gamma_1}, \Pi_2 \circ \Phi_{\Gamma_2}) \leq 2\sqrt{NTw_{\Pi, \text{out}}B_{\Pi}2^{-M}} \\ \Pi_1 \circ \Phi_{\Gamma_1}, \Pi_2 \circ \Phi_{\Gamma_2} \in \mathcal{F}_{\Pi \circ \Phi_{\Gamma}}} } \kappa(\Pi_1 \circ \Phi_{\Gamma_1}, \tilde{\sigma}) - \kappa(\Pi_2 \circ \Phi_{\Gamma_2}, \tilde{\sigma}) \\ &+ 4\sqrt{2} \int_{\sqrt{NTw_{\Pi, \text{out}}B_{\Pi}2^{-M}}}^{\sqrt{NTw_{\Pi, \text{out}}B_{\Pi}}} \sqrt{\ln N(\mathcal{F}_{\Pi \circ \Phi_{\Gamma}}, d_k, \varepsilon)} d\varepsilon. \end{aligned} \quad (\text{B.5})$$

Since M are arbitrary and the outputs of $\forall \Pi \circ \Phi_{\Gamma} \in \mathcal{F}_{\Pi \circ \Phi_{\Gamma}}$ are all continuous functions, under M approaching the positive infinity, the first term on the right side of Eq. (B.5) converges to zero, yielding

$$\mathbb{E}_{\tilde{\sigma}} \sup_{\Pi \circ \Phi_{\Gamma} \in \mathcal{F}_{\Pi \circ \Phi_{\Gamma}}} \kappa(\Pi \circ \Phi_{\Gamma}, \tilde{\sigma}) \leq 4\sqrt{2} \int_0^{\sqrt{NTw_{\Pi, \text{out}}B_{\Pi}}} \sqrt{\ln N(\mathcal{F}_{\Pi \circ \Phi_{\Gamma}}, d_k, \varepsilon)} d\varepsilon. \quad (\text{B.6})$$

This completes the proof. ■

Appendix C. Approach for Training the Neural Oscillator

By introducing the state space vector $\mathbf{z}(t) = [\mathbf{z}_1^\top(t), \mathbf{z}_2^\top(t)]^\top = [\mathbf{x}^\top(t), \mathbf{x}'^\top(t)]^\top$, Eq. (1) over the time interval $[0, T]$ can be rewritten in the state function form

$$\begin{cases} \mathbf{z}'_1(t) = \mathbf{z}_2(t) \\ \mathbf{z}'_2(t) = \Gamma[\mathbf{z}_1(t), \mathbf{z}_2(t), \mathbf{u}(t)]. \\ \mathbf{y}(t) = \Pi[\mathbf{z}_1(t), \mathbf{u}(0), t] \end{cases} \quad (\text{C.1})$$

Utilizing a second-order Runge-Kutta scheme (Griffiths and Higham, 2010), a time-discretization form of Eq. (C.1) is

$$\begin{cases} \mathbf{y}(t_{i+1}) = \Pi[\mathbf{z}_1(t_{i+1}), \mathbf{u}(0), t_{i+1}] \\ \mathbf{z}(t_{i+1}) = 0.5\Delta t_i(\mathbf{k}_2 + \mathbf{k}_1) \\ \mathbf{k}_2 = \left\{ \begin{array}{l} \mathbf{z}_2(t_i) + \Delta t_i \mathbf{k}_{12} \\ \Gamma[\mathbf{z}_1(t_i) + \Delta t_i \mathbf{k}_{11}, \mathbf{z}_2(t_i) + \Delta t_i \mathbf{k}_{12}, \mathbf{u}(t_{i+1})] \end{array} \right\} \\ \mathbf{k}_1 = \begin{bmatrix} \mathbf{k}_{11} \\ \mathbf{k}_{12} \end{bmatrix} = \left\{ \begin{array}{l} \mathbf{z}_2(t_i) \\ \Gamma[\mathbf{z}_1(t_i), \mathbf{z}_2(t_i), \mathbf{u}(t_i)] \end{array} \right\} \end{cases} \quad (\text{C.2})$$

where $\mathbf{z}(0) = \mathbf{0}$, $\mathbf{y}(0) = \Pi[\mathbf{z}_1(0), \mathbf{u}(0), t]$, $\Delta t_i = t_{i+1} - t_i$, $0 = t_0 < t_1 < t_2 < \dots < t_L = T$. Given available output function samples $\hat{\mathbf{y}}_l(t_i) = [\hat{y}_{l,1}(t_i), \hat{y}_{l,2}(t_i), \dots, \hat{y}_{l,q}(t_i)]^\top$ caused by the input samples $\mathbf{u}_l(t_i)$, $l = 1, 2, \dots, L$, the loss function $\hat{\ell}_{\lambda_L}$ is used to learn the parameters of the MLPs $\Gamma(\cdot)$ and $\Pi(\cdot)$ in Eq. (C.1),

$$\hat{\ell}_{\lambda_L} = \frac{1}{LIq} \sum_{l=1}^L \sum_{i=0}^{L-1} \sum_{j=1}^q |y_{l,j}(t_i) - \hat{y}_{l,j}(t_i)|^2 + \frac{\lambda_L}{\sqrt{N}} \left[\sum_{i=1}^2 (|\mathbf{W}_{i1,1}| + |\mathbf{b}_{i1}|) + \sum_{j=1}^{h_{\Pi}} (|\tilde{\mathbf{W}}_{j1,1}| + |\tilde{\mathbf{b}}_{j1}|) \right], \quad (\text{C.3})$$

where $\mathbf{y}_l(t_i) = [y_{l,1}(t_i), y_{l,2}(t_i), \dots, y_{l,q}(t_i)]^\top$ represents the output computed from the neural oscillator driven by $\mathbf{u}_l(t_i)$ using Eq. (C.2). In this numerical study, the Adam method (Kingma and Ba, 2014) implemented using the PyTorch (Paszke et al., 2019) is utilized to train the neural oscillator using the Runge-Kutta scheme in Eq. (C.2) and the loss function $\hat{\ell}_{\lambda_L}$ in Eq. (C.3).

References

- Adcock, B., Griebel, M., Maier, G., 2025. The sample complexity of learning lipschitz operators with respect to gaussian measures. URL: <https://arxiv.org/abs/2410.23440>, arXiv:2410.23440.
- Ames, W.F., Pachpatte, B., 1997. Inequalities for differential and integral equations. volume 197. Elsevier.

- Bartlett, P., 2013. Theoretical statistics: Lecture 14. <https://www.stat.berkeley.edu/~bartlett/courses/2013spring-stat210b/notes/14notes.pdf>.
- Bartlett, P.L., Foster, D.J., Telgarsky, M.J., 2017. Spectrally-normalized margin bounds for neural networks. *Advances in neural information processing systems* 30.
- Beattie, R., Butzmann, H.P., 2013. *Convergence structures and applications to functional analysis*. Springer Science & Business Media.
- Bleistein, L., Guilloux, A., 2023. On the generalization and approximation capacities of neural controlled differential equations. *arXiv preprint arXiv:2305.16791* .
- Chen, M., Li, X., Zhao, T., 2020. On generalization bounds of a family of recurrent neural networks, in: *International Conference on Artificial Intelligence and Statistics*, PMLR. pp. 1233–1243.
- Cho, K., Van Merriënboer, B., Gulcehre, C., Bahdanau, D., Bougares, F., Schwenk, H., Bengio, Y., 2014. Learning phrase representations using rnn encoder-decoder for statistical machine translation. *arXiv preprint arXiv:1406.1078* .
- Fermanian, A., Marion, P., Vert, J.P., Biau, G., 2021. Framing rnn as a kernel method: A neural ode approach. *Advances in Neural Information Processing Systems* 34, 3121–3134.
- Foucart, S., Rauhut, H., 2013. *A Mathematical Introduction to Compressive Sensing*. Applied and Numerical Harmonic Analysis, Springer New York. URL: <https://books.google.com.hk/books?id=zb28BAAAQBAJ>.
- Fung, S.W., Berkels, B., 2024. A generalization bound for a family of implicit networks. *arXiv preprint arXiv:2410.07427* .
- Gonon, L., Grigoryeva, L., Ortega, J.P., 2020. Risk bounds for reservoir computing. *Journal of Machine Learning Research* 21, 1–61.
- Gonon, L., Grigoryeva, L., Ortega, J.P., 2023. Approximation bounds for random neural networks and reservoir systems. *The Annals of Applied Probability* 33, 28–69.
- Gouk, H., Frank, E., Pfahringer, B., Cree, M.J., 2021. Regularisation of neural networks by enforcing lipschitz continuity. *Machine Learning* 110, 393–416.
- Griffiths, D.F., Higham, D.J., 2010. *Numerical methods for ordinary differential equations: initial value problems*. volume 5. Springer.
- Grigoryeva, L., Ortega, J.P., 2018a. Echo state networks are universal. *Neural Networks* 108, 495–508.
- Grigoryeva, L., Ortega, J.P., 2018b. Universal discrete-time reservoir computers with stochastic inputs and linear readouts using non-homogeneous state-affine systems. *Journal of Machine Learning Research* 19, 1–40.
- Gu, A., Dao, T., 2023. Mamba: Linear-time sequence modeling with selective state spaces. *arXiv preprint arXiv:2312.00752* .
- Gu, A., Dao, T., Ermon, S., Rudra, A., Ré, C., 2020. Hippo: Recurrent memory with optimal polynomial projections. *Advances in neural information processing systems* 33, 1474–1487.
- Gu, A., Goel, K., Gupta, A., Ré, C., 2022. On the parameterization and initialization of diagonal state space models. *Advances in Neural Information Processing Systems* 35, 35971–35983.
- Gu, A., Goel, K., Ré, C., 2021. Efficiently modeling long sequences with structured state spaces. *arXiv preprint arXiv:2111.00396* .
- Hanin, B., 2019. Universal function approximation by deep neural nets with bounded width and relu activations. *Mathematics* 7, 992.

- Hanson, J., Raginsky, M., 2020. Universal simulation of stable dynamical systems by recurrent neural nets, in: Learning for Dynamics and Control, PMLR. pp. 384–392.
- Hanson, J., Raginsky, M., 2024. Rademacher complexity of neural odes via chen-fliess series, in: 6th Annual Learning for Dynamics & Control Conference, PMLR. pp. 758–769.
- Hanson, J., Raginsky, M., Sontag, E., 2021. Learning recurrent neural net models of nonlinear systems, in: Learning for Dynamics and Control, PMLR. pp. 425–435.
- He, K., Zhang, X., Ren, S., Sun, J., 2015. Delving deep into rectifiers: Surpassing human-level performance on imagenet classification, in: Proceedings of the IEEE international conference on computer vision, pp. 1026–1034.
- Hochreiter, S., Schmidhuber, J., 1997. Long short-term memory. *Neural computation* 9, 1735–1780.
- Hoffman, J., Roberts, D.A., Yaida, S., 2019. Robust learning with jacobian regularization. arXiv preprint arXiv:1908.02729 .
- Honarpisheh, A., Bozdag, M., Camps, O., Sznaier, M., 2025. Generalization error analysis for selective state-space models through the lens of attention. The Thirty-ninth Annual Conference on Neural Information Processing Systems URL: <https://openreview.net/forum?id=YVZbaVikBp>.
- Huang, Z., Xia, Y., 2022. Probability distribution estimation for harmonisable loads and responses of linear elastic structures. *Probabilistic Engineering Mechanics* 68, 103258.
- Huang, Z., Xia, Y., 2025. Universal runge–kutta neural oscillator for stochastic response analysis of nonlinear dynamic systems under random loads. *Journal of Engineering Mechanics* 151, 04025033.
- Huang, Z., Zuev, K.M., Xia, Y., Beer, M., 2025. Upper approximation bounds for neural oscillators. arXiv preprint arXiv:2512.01015 .
- Kingma, D.P., Ba, J., 2014. Adam: A method for stochastic optimization. arXiv preprint arXiv:1412.6980 .
- Kovachki, N., Li, Z., Liu, B., Azzadenesheli, K., Bhattacharya, K., Stuart, A., Anandkumar, A., 2023. Neural operator: Learning maps between function spaces with applications to pdes. *Journal of Machine Learning Research* 24, 1–97.
- Lanthaler, S., 2024. Operator learning of lipschitz operators: An information-theoretic perspective. arXiv preprint arXiv:2406.18794 .
- Lanthaler, S., Rusch, T.K., Mishra, S., 2023. Neural oscillators are universal. *Advances in Neural Information Processing Systems* 36, 46786–46806.
- Li, Z., Han, J., E, W., Li, Q., 2022. Approximation and optimization theory for linear continuous-time recurrent neural networks. *Journal of Machine Learning Research* 23, 1–85. URL: <http://jmlr.org/papers/v23/21-0368.html>.
- Liu, F., Li, Q., 2024. From generalization analysis to optimization designs for state space models, in: International Conference on Machine Learning, PMLR. pp. 31383–31405.
- Liu, H.T.D., Williams, F., Jacobson, A., Fidler, S., Litany, O., 2022. Learning smooth neural functions via lipschitz regularization, in: ACM SIGGRAPH 2022 Conference Proceedings, pp. 1–13.
- Marion, P., 2023. Generalization bounds for neural ordinary differential equations and deep residual networks. *Advances in Neural Information Processing Systems* 36, 48918–48938.
- Maurer, A., 2016. A vector-contraction inequality for rademacher complexities, in: Algorithmic Learning Theory: 27th International Conference, ALT 2016, Bari, Italy, October 19-21, 2016, Proceedings 27, Springer. pp. 3–17.

- Mohri, M., Rostamizadeh, A., Talwalkar, A., 2018. Foundations of Machine Learning, second edition. Adaptive Computation and Machine Learning series, MIT Press. URL: <https://books.google.com.hk/books?id=V2B9DwAAQBAJ>.
- Nair, V., Hinton, G.E., 2010. Rectified linear units improve restricted boltzmann machines, in: Proceedings of the 27th international conference on machine learning (ICML-10), pp. 807–814.
- Orvieto, A., De, S., Gulcehre, C., Pascanu, R., Smith, S.L., 2024. Universality of linear recurrences followed by non-linear projections: Finite-width guarantees and benefits of complex eigenvalues, in: International Conference on Machine Learning, PMLR. pp. 38837–38863.
- Pascanu, R., Mikolov, T., Bengio, Y., 2013. On the difficulty of training recurrent neural networks, in: International conference on machine learning, Pmlr. pp. 1310–1318.
- Paszke, A., Gross, S., Massa, F., Lerer, A., Bradbury, J., Chanan, G., Killeen, T., Lin, Z., Gimelshein, N., Antiga, L., et al., 2019. Pytorch: An imperative style, high-performance deep learning library. Advances in neural information processing systems 32.
- Rácz, D., Petreczky, M., Daróczy, B., 2024. Length independent generalization bounds for deep ssm architectures, in: Next Generation of Sequence Modeling Architectures Workshop at ICML 2024.
- Rumelhart, D.E., Hinton, G.E., Williams, R.J., 1986. Learning representations by back-propagating errors. nature 323, 533–536.
- Rusch, T.K., Mishra, S., 2020. Coupled oscillatory recurrent neural network (cornn): An accurate and (gradient) stable architecture for learning long time dependencies. arXiv preprint arXiv:2010.00951 .
- Rusch, T.K., Mishra, S., 2021. Unicorn: A recurrent model for learning very long time dependencies, in: International Conference on Machine Learning, PMLR. pp. 9168–9178.
- Rusch, T.K., Rus, D., 2024. Oscillatory state-space models. arXiv preprint arXiv:2410.03943 .
- Shalev-Shwartz, S., Ben-David, S., 2014. Understanding machine learning: From theory to algorithms. Cambridge university press.
- Strogatz, S.H., 2024. Nonlinear dynamics and chaos: with applications to physics, biology, chemistry, and engineering. Chapman and Hall/CRC.
- van der Vaart, A.W., Wellner, J.A., 2013. Weak Convergence and Empirical Processes: With Applications to Statistics. Springer Series in Statistics, Springer New York. URL: <https://books.google.com.hk/books?id=zDkBwAAQBAJ>.
- Vaswani, A., Shazeer, N., Parmar, N., Uszkoreit, J., Jones, L., Gomez, A.N., Kaiser, Ł., Polosukhin, I., 2017. Attention is all you need. Advances in neural information processing systems 30.
- Wei, C., Ma, T., 2019. Data-dependent sample complexity of deep neural networks via lipschitz augmentation. Advances in neural information processing systems 32.
- Yasumoto, H., Tanaka, T., 2025. Universality of reservoir systems with recurrent neural networks. Neural Networks 188, 107413.
- Yoshida, Y., Miyato, T., 2017. Spectral norm regularization for improving the generalizability of deep learning. arXiv preprint arXiv:1705.10941 .